Front. Optoelectron. 2016, 9(1): 3–37
DOI 10.1007/s12200-016-0563-x

REVIEW ARTICLE

Donor design and modification strategies of metal-free sensitizers for highly-efficient n-type dye-sensitized solar cells

Xiaoyu ZHANG[1,2], Michael Grätzel[2], Jianli HUA (✉)[1]

1 Key Laboratory for Advanced Materials and Institute of Fine Chemicals, East China University of Science and Technology, Shanghai 200237, China

2 Laboratoire de Photoniques et Interfaces, Institut des Sciences et Ingénierie Chimiques, École Polytechnique Fédérale de Lausanne, Lausanne, Switzerland

Abstract Dye-sensitized solar cells (DSSCs) cannot be developed without the research on sensitizers. As the key of light harvesting and electron generation, thousands of sensitizers have been designed for the application in DSSC devices. Among them, organic sensitizers have drawn a lot of attention because of the flexible molecular design, easy synthesis and good photovoltaic performance. Recently, new record photovoltaic conversion efficiencies of 11.5% for DSSCs with iodide electrolyte and 14.3% for DSSCs with cobalt electrolyte and co-sensitization have been achieved with organic sensitizers. Here we focus on the donor design and modification of organic sensitizers. Several useful strategies and corresponding typical examples are presented.

Keywords donors, organic sensitizers, dye-sensitized solar cells (DSSCs)

1 Introduction

The world's energy crisis has forced and accelerated the development of many renewable energy technologies, among which the solar cell is regard as one of the most promising technologies due to its clean and abundant energy resource. Dye-sensitized solar cells (DSSCs) have been intensively studied as one of the third-generation solar cells for its potential for roll-to-roll mass production, cost-efficient and easy fabrication procedures, colorful appearance and high solar-to-electricity conversion efficiency even under low light intensity [1–3]. Having been developed for more than two decades, DSSCs have already achieved the photovoltaic conversion efficiency (η) as high as 14.3% with an alkoxysilyl-anchor organic dye co-sensitizing with a carboxy-anchor organic dye in cooperate with cobalt complex-based redox electrolyte, which is tempting for industrial applications of DSSCs [4]. Since the first report of the DSSC in 1991 [5], the device structure and working principles of a typical DSSC have not changed so much. There are several important components: 1) the transparent conducting glass. For DSSCs, fluorine-doped SnO_2 (FTO) glass is the most commonly-used substrate due to its chemical inertness and high-temperature resistance; 2) the mesoporous semiconductor film, normally TiO_2; 3) the sensitizers that absorbed on the surface of mesoporous semiconductor layer. Sensitizers are crucial to the photovoltaic performance of DSSCs because they are the key of converting solar energy into electricity; 4) the redox electrolyte, which is very important for regenerating dyes and completing the electronic circuit; 5) the counter electrode. Normally for liquid-state DSSCs, the counter electrode is made by depositing catalyst of the redox couples (such as platinum or carbon materials) on the top of FTO glass. Figure 1 shows the device structure and working principle of a typical DSSC.

When the sunlight illuminates on a DSSC, the dyes (D) harvest photons and reach excited states (D*). The electrons are injected into the conductive band (CB) of TiO_2 due to the energy level difference between $E_{(D+/D^*)}$ and E_{CB}, and flow into the external circuit, generating the photocurrent. Then the oxidized dyes are regenerated by the reductive species of redox couples. The oxidized species of redox couples will diffuse to the counter electrode to get electrons and complete the whole electronic circuit. The energy level diagram and electron

Received November 16, 2015; accepted December 10, 2015

E-mail: jlhua@ecust.edu.cn

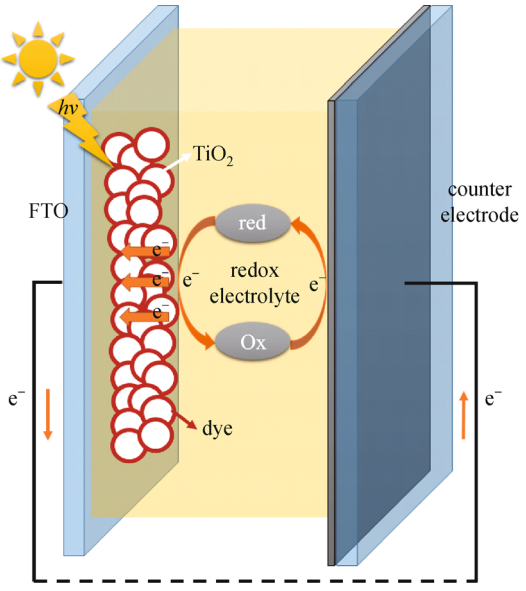

Fig. 1 A simple model for device and working principles of a typical DSSC

transfer processes of DSSCs are demonstrated clearly in Fig. 2. The green arrows show the routes of electrons inside a working DSSC, representing the process of light harvesting and excitation of the dyes (Arrow 1), electron injection (Arrow 2), dye regeneration (Arrow 3), excited state decay (Arrow 4), charge recombination of electrons in the mesoporous semiconductor films with oxidized dyes (Arrow 5) or oxidized species in the electrolyte (Arrow 6). Process 4, 5 and 6 pose a negative effect on the solar-to-electricity conversion, which we shall minimize through device and material optimization.

As shown in Fig. 2, the open-circuit voltage (V_{oc}) is determined by the difference between the quasi Fermi energy level of TiO_2 and the redox potential of electrolyte. The formula is as follows [10]:

$$V_{oc} = \frac{E_{CB}}{q} + \frac{kT}{q}\ln\left(\frac{n}{N_{CB}}\right) - \frac{E_{redox}}{q}, \quad (1)$$

where E_{CB} is the CB energy level of TiO_2, q is the unit electron charge, n is the number of electrons in the TiO_2 film, N_{CB} is the accessible density of states and E_{redox} is the redox potential of redox couples.

Another crucial parameter of the device photovoltaic performance is short-circuit current density (J_{sc}). It corresponds to the incident photon-to-current conversion efficiency (IPCE) of the DSSC, which can be expressed as the product of light harvesting efficiency (LHE), electron injection efficiency (η_{inj}), charge collection efficiency (η_{col}) and dye regeneration efficiency (η_{reg}) [11]:

$$\mathrm{IPCE}(\lambda) = \mathrm{LHE}(\lambda) \times \eta_{inj} \times \eta_{col} \times \eta_{reg}. \quad (2)$$

And the LHE at a certain wavelength is defined as [12]

$$\mathrm{LHE}(\lambda) = 1 - 10^{-A}, \quad (3)$$

where A is the absorbance of dye-sensitized semiconductor film, which is related to the molar extinction coefficient (ε) and dye loading amount.

The photovoltaic conversion efficiency (PCE) of a DSSC can be obtained via the following equation [13]:

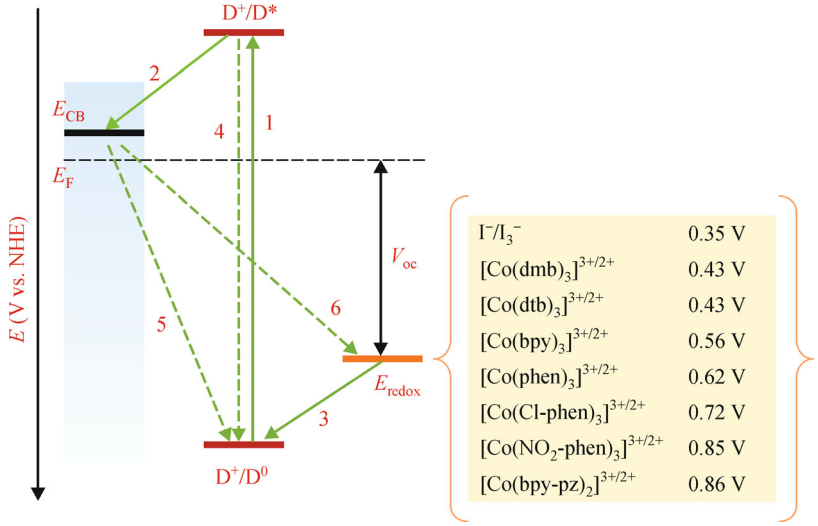

Fig. 2 Energy level diagram and electron transfer processes in a typical DSSC device (vs. the normal hydrogen electrode, NHE). The insert shows several redox potential examples of redox couples: I^-/I_3^-, iodide/triiodide, Ref. [6]; $[Co(dmb)_3]^{3+/2+}$, cobalt(II/III) tris(4,4′-dimethyl-2,2′-bipyridine) complexes, $[Co(dtb)_3]^{3+/2+}$, cobalt(II/III) tris(4,4′-ditert-butyl-2,2′-bipyridine) complexes, $[Co(bpy)_3]^{3+/2+}$, cobalt (II/III) tris(2,2′-bipyridine) complexes, $[Co(phen)_3]^{3+/2+}$, cobalt(II/III) tris(1,10-phenanthroline) complexes, Ref. [7]; $[Co(Cl\text{-}phen)_3]^{3+/2+}$, cobalt(II/III) tris(5-chloro-1,10-phenanthroline) complexes, $[Co(NO_2\text{-}phen)_3]^{3+/2+}$, cobalt(II/III) tris(5-nitro-1,10-phenanthroline) complexes, Ref. [8]; $[Co(bpy\text{-}pz)_2]^{3+/2+}$, cobalt(II/III) bis[6-(1*H*-pyrazol-1-yl)-2,2′-bipyridine] complexes, Ref. [9]

$$\mathrm{PCE} = \frac{J_{sc} \times V_{oc} \times FF}{P_{in}}, \quad (4)$$

where P_{in} is the incident light intensity, *FF* is the fill factor which is defined as the ratio of the maximum power (P_{max}= $J_{max} \times V_{max}$) of the DSSC, and the product of J_{sc} and V_{oc}, that is

$$FF = \frac{J_{max} \times V_{max}}{J_{sc} \times V_{oc}}. \quad (5)$$

Therefore, for the aim of obtaining high photovoltaic conversion efficiency, high J_{sc} and V_{oc} are necessary. There are several general ways to improve V_{oc}: 1) using redox shuttles with more positive redox potentials. I^-/I_3^- is the most traditional redox couple used in DSSCs owing to their desirable kinetic properties and high carrier collection efficiencies [6]. However, the standard potential of I^-/I_3^- redox couple is 0.35 V vs. NHE, which limits the open-circuit voltage. Many alternative redox couples have been applied to DSSCs for the purpose of getting a higher V_{oc} [14]. Some examples and their redox potentials have been displayed in Fig. 2; 2) adding additives to shift the conduction band of TiO_2, such as *tert*-butylpyridine (TBP) [15]; 3) optimizing the device and materials to retard the charge recombination of electrons in the photoanode with oxidized dyes and oxidized species in redox electrolyte at the interfaces of TiO_2/dye/electrolyte and FTO/electrolyte as well as to reduce the dye aggregation which could cause the self-quenching effect [16–18].

For DSSCs with a given redox electrolyte, the V_{oc} will not change too much thus the enhancement of J_{sc} is very important. That is the one of the reason why researchers are trying so hard for searching a well-performed dye with broad spectral response, high molar extinction coefficient, matched energy levels and good stability [19,20]. For now, the high efficient sensitizers employed in DSSCs can be roughly categorized into three groups: ruthenium dyes, porphyrin dyes and metal-free organic dyes. All of them have already been reported with device PCEs above 11% [4,21–26]. Compared with ruthenium dyes and porphyrin dyes, metal-free organic dyes have many advantages such as great flexibility in molecular design for fine tuning the optical and electrochemical properties, high molar extinction coefficient as well as low-cost and easy synthesis [27]. In general, a metal-free organic dye is consist of donor (D), π-bridge (π) and acceptor (A) due to the good intramolecular charge transfer (ICT) property. When the dye absorbs a photon, the donor part gives an electron, which goes through the π-bridge to the acceptor for the push and pull effect [28]. Then the electron is injected into the TiO_2 film. Different donors, π-bridges and acceptors and their influence on properties and device performance have been studied by many research groups. Some common units of donors, π-bridges and acceptors are displayed in Fig. 3. Donor is an important part where the electrons are generated. In this review, we are going to focus on the donor designs and modifications of organic sensitizers for highly-efficient n-type DSSCs with iodide electrolyte and cobalt electrolyte.

2 Strategies for donor design and modification in traditional DSSCs with iodide electrolyte

2.1 Use properly strong electron-donating group or planar donor to broad the spectral response

The electron-donating ability of a donor is a primary consideration since it is not only closely related to the light harvesting capacity but also the energy levels of the sensitizer, thus plays an important role in the generation of photocurrent and charge transfer kinetics at the interface of TiO_2/dye/electrolyte such as dye regeneration and recombination processes [29]. Many groups have investigated different donors and their relationships between device performances (Scheme 1). Our group compared *N*, *N*-dialkylaniline (Dye **1**), triphenylamine (Dye **2**) and indoline (Dye **3**) as donor part with an isophorone-incorporated π-conjugation system. Results show that indoline as donor is more favorable than *N*, *N*-dialkylaniline and triphenylamine. Not only the maximum absorption wavelength was largely red-shifted but also the molar extinction coefficient was increased. Finally, the highest PCE of 7.41% was achieved with **3** under AM 1.5 illumination with a much higher J_{sc} of 18.63 mA/cm^2 than that of **1** (J_{sc} = 12.33 mA/cm^2) and **2** (J_{sc} = 11.46 mA/cm^2). DSSC based on **2** with triphenylamine as donor performed slightly worse than that of **1** with *N*, *N*-dimethylaniline. The J_{sc} of DSSC based on **2** was lower for the blue-shifted absorption peak and lower molar extinction coefficient. The sequence of electron donating ability of these three donor are as follows: indoline > *N*, *N*-dimethylaniline > triphenylamine, which is in accordance with their dye properties and device performance [30]. However, donor with stronger electron-donating ability does not always result in higher PCE. Xue's group also studied *N*, *N*-dimethylaniline (Dye **4**) and triphenylamine (Dye **5**) in a system of cyclopentadithiophene (CPDT) as the π-bridge. Even though *N*, *N*-dimethylaniline as donor still offered a broader absorption range than its triphenylamine analog, the molar extinction coefficient of **4** is less than **5**'s. With the co-adsorption of 1.5 mM[1)] chenodeoxycholic acid (CDCA), DSSC sensitized by **5** gave higher PCE of 6.3% with J_{sc} = 15.2 mA/cm^2 than that of **4** with PCE = 5.7% and J_{sc} = 13.7 mA/cm^2 [31]. The authors explained that *N*, *N*-dimethylaniline cannot provide enough steric hindrance to suppress charge recombination when CPDT was used as π-

1) 1 mM = 1 mmol/L

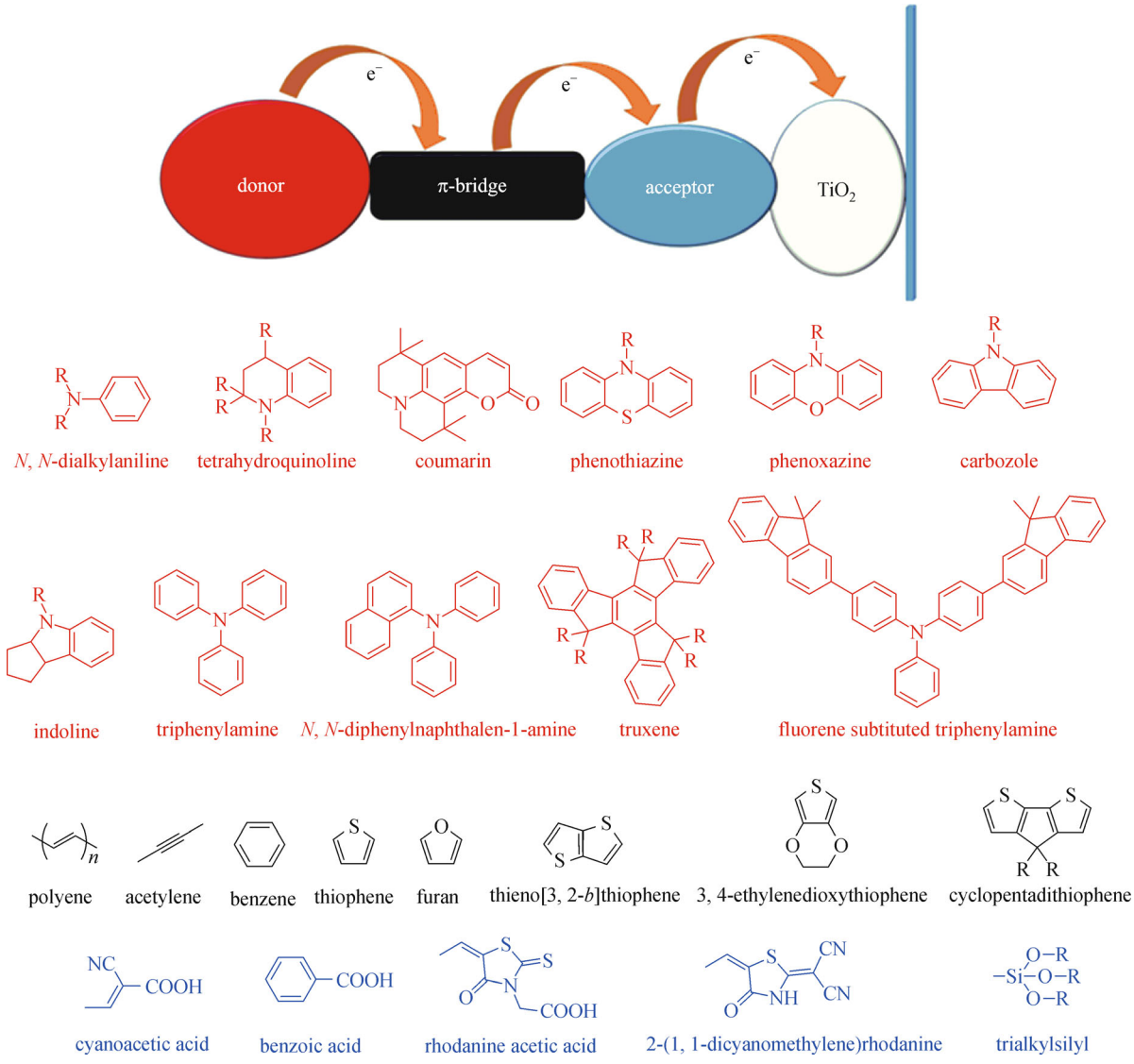

Fig. 3 A model for D-π-A structure and common groups for donor, π-bridge and acceptor part

bridge, which is different with our system since the isophorone was specially chosen to provide steric hindrance. Therefore, the optical and electrochemical properties and device performance cannot be simply judged by the electron-donating capability because they are affected by every segment of the dye and also the condition of device fabrication.

Chang and Chow made a very careful investigation about the effect of donor changing. Comparing dye **6** and dye **10** with their corresponding triphenylamine anologues dye **7** and dye **11**, they found that by replacing one phenyl with naphthalene group, the molar extinction coefficients increased largely. While for replacing one phenyl with thiophene, the outcomes were quite different. Thiophene has a lower oxidation potential than phenyl unit, which can cause the bathochromic shift of absorption peaks. However, the molar extinction coefficients dropped. What's more, the strong electron-donating abilities of *N*-(naphthalen-1-yl)-*N*-phenylthiophen-2-amine and *N*, *N*-diphenylthiophen-2-amine pushed the highest occupied molecular orbital (HOMO) energy level so high (0.53 V vs. NHE for **10** and 0.58 V vs. NHE for **11**) that the driving force of dye regeneration might not be enough anymore, resulting a low IPCE, which affects the power conversion efficiency directly. In the end, the highest PCE of 7.08% was obtained by DSSC based on **6** while **11** and **10** only provided PCEs of 3.75% and 3.74%, respectively. Therefore, the electron-donating ability of the donor is not the case that the stronger the better. Donor with too strong electron-donating capability will result in a large negative shift of HOMO energy level, which might cause the mismatch of energy levels and jeopardize the device performance [32].

Bridged triphenylamine as a new donor has been introduced into organic sensitizers. The planar structure can improve the electron delocalization on the donor,

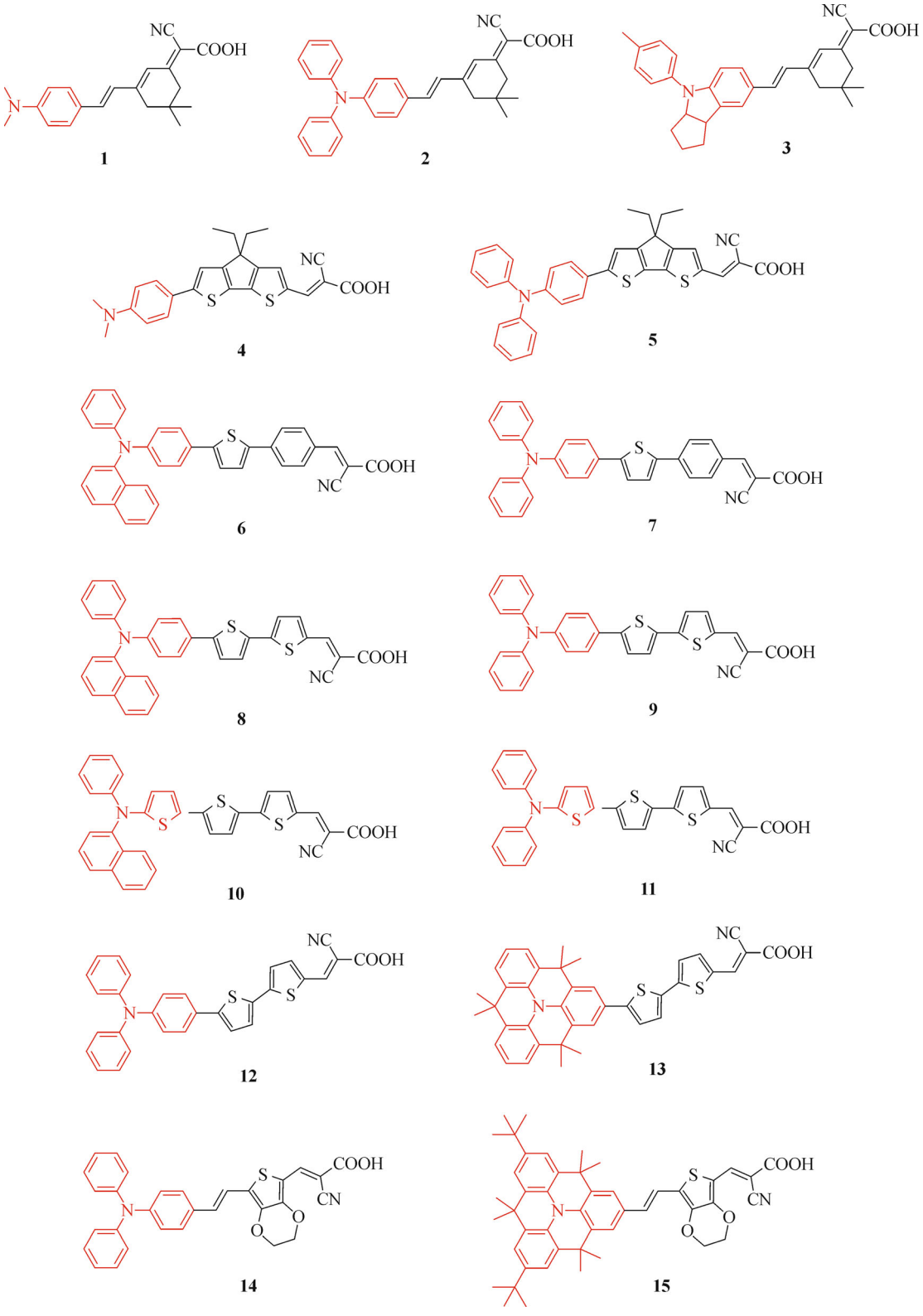

Scheme 1 Molecular structures of dyes **1**–**15**

which can lead to a large bathochromic shift of the absorption peak. Ko and his colleagues designed and synthesized dyes with bridged triphenylamine. Compared with its triphenylamine analog **12**, **13** showed a red-shifted absorption band. The IPCE of **13** exceeded 80% over the wavelength region from 400 to 600 nm and reached 90% at 485 nm, providing J_{sc} of 15.2 mA/cm^2 which was higher than 13.0 mA/cm^2 for DSSC based on **12**. In the end, DSSC based on **13** reached PCE of 7.87% in contrast to PCE of 6.00% obtained by DSSC based on **12** in the same conditions [33].

Another successful example is presented by Liu's group and Grätzel's group. They synthesized dye **15** with *tert*-butyl-substituted bridged triphenylamine as the donor and compared with its triphenylamine analog **14**. Large enhancements on molar extinction coefficient and maximum absorption wavelength were observed, leading to big improvements of J_{sc} from 8.92 mA/cm^2 (**14**) to 15.37 mA/cm^2 (**15**) and PCE from 4.44% (**14**) to 7.51% (**15**) [34].

2.2 Expand donor part with additional electron-donating units to broaden the spectral response

One easy approach to increase the electron-donating ability of donor part is simply to expand the donor with additional electron-donating units (Scheme 2), thus forming a D-D-π-A configuration. Since our first report on starburst D-D-π-A sensitizer **16** exhibiting a good device performance of 6.02% in 2008 [35], many D-D-π-A sensitizers have been developed and applied to DSSCs by different groups. Wan and his colleagues compared effect of phenothiazine (**17**) and carbazole (**18**) as antenna in the starburst dyes. The results showed that phenothiazine as antenna had better contribution to improve the electron-donating ability than carbazole. The high molar extinction coefficient of **17** was consistent with the higher IPCE, leading to higher J_{sc} of 9.2 mA/cm^2 and PCE of 4.54% whereas J_{sc} of 7.3 mA/cm^2 and PCE of 3.26% for **18** in DSSCs [36]. By introducing one or two 4-(*p*-tolyl)-1,2,3,3a,4,8b-hexahydrocyclopenta [b]indole as additional donor moiety onto the triphenylamine part of reference dye **19**, **20** and **21** displayed red-shifted absorption peaks, increased molar extinction coefficients and positively shifted HOMO energy levels. Further investigation found out that the two indoline segments spreading out from triphenylamine can increase the possibility of interacting with the adjacent molecules and result in excited-state self-quenching. The IPCE curve of DSSC based on **21** without any coadsorbent was below 30%, which was magnificently enhanced to almost 70% after adding 5 mM CDCA. The DSSC devices with 5 mM CDCA based on **20** and **21** showed higher PCEs (6.38% for **20** and 5.99% for **21**) and J_{sc}s (11.33 mA/cm^2 for **20** and 11.15 mA/cm^2 for **21**) than that of **19** (5.45%, 9.72 mA/cm^2) [37].

Since heterocyclic groups containing electron-rich atoms such as sulfur or nitrogen also have good electron-donating properties, Zhang and his coworkers adopted 2-thienyl and 1-pyrazolyl and added them onto triphenylamine donor of dye **22**, offering two new dyes **23** and **24**, respectively. Calculated HOMO levels of **23** and **24** showed good electron distributions on the heterocyclic substituted triphenylamine donor parts. Compared to **22**, the absorption peaks of **23** and **24** were red-shifted and higher molar extinction coefficients were also obtained, which were responsible for the ca. 31% enhancement of short-circuit current density. PCEs of **23**- and **24**-sensitized DSSCs were 5.21% and 4.92%, respectively, higher than PCE of 3.80% for **22** [38].

D-D-π-A can also be constructed in simple linear structure. For example, our group extended phenothiazine dyes by adding CH_3O- substituted triphenylamine (**25**), triphenylamine (**26**) and 1,1,2-triphenylethene (**27**). The maximum absorption wavelengths of these three dyes were almost the same but **26** had the highest molar extinction coefficient which benefited its light harvesting, thus gave the best J_{sc} of 10.84 mA/cm^2, resulting the highest PCE of 4.41% [39].

Liu and his coworkers introduced an additional donor group into the indoline unit in the donor part to increase the electron-donating ability of the donor part (Scheme 3). 4-Methylphenyl, carbazole and fluorene were adopted to form three D-D-π-A dyes (**28**, **29** and **30**, respectively). As expected, the absorption peaks of **29** and **30** were red-shifted by 32 and 13 nm compared with that of **28**. So did their molar extinction coefficients increased. DSSC based on **29** with strong electron-donating carbazole unit as additional donor exhibited a broad IPCE spectrum stretching into near infrared (NIR) region. With the co-absorbance of 30 mM deoxycholic acid (DCA), DSSCs based on **29**, **30** and **28** displayed the J_{sc}s of 18.53, 15.29 and 11.63 mA/cm^2, respectively, which were in good accordance with their light-harvesting abilities. In the end, DSSCs based on **29**, **30** and **28** yielded the PCEs of 8.49%, 6.84% and 5.08%, respectively, proving that constructing D-D-π-A sensitizers with suitable additional electron-donating units is an effective approach to increase light-harvesting capability and overall solar cell efficiency [40]. After optimization the π-bridge of **29** with thiophene (**31**) and furan (**32**), the device performance was improved further to 9.29% and 9.49%, respectively, for the increased photovoltage by removing the vinyl bond [41].

Xue's group also constructed a series of indoline based D-D-π-A sensitizers with different additional donors like dipropylfluorene (**33**), hexyloxybenzene (**34**), *tert*-butylbenzene (**35**), and hexapropyltruxene (**36**). **33** and **34** had better light harvesting ability compared to **35** and **36**, contributing to their slightly higher J_{sc}. With the co-absorption with a small triphenylamine-based dye, the dye aggregation was further impeded. Increments in V_{oc} and J_{sc} led to the high PCEs of **33**, **34**, **35** and **36** as 8.18%, 7.06%, 7.36 and 8.08%, respectively [42].

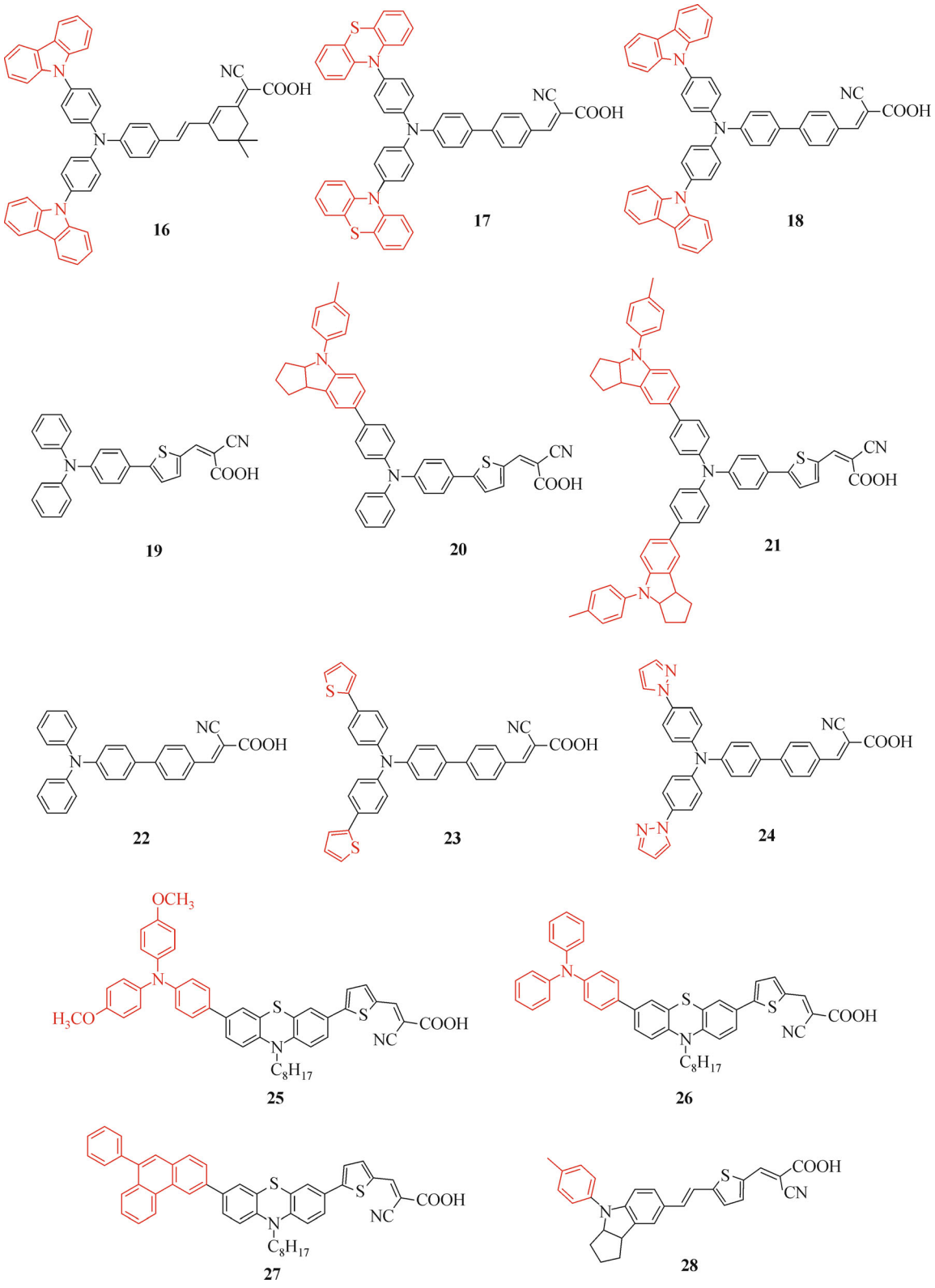

Scheme 2 Molecular structures of dyes **16**–**28**

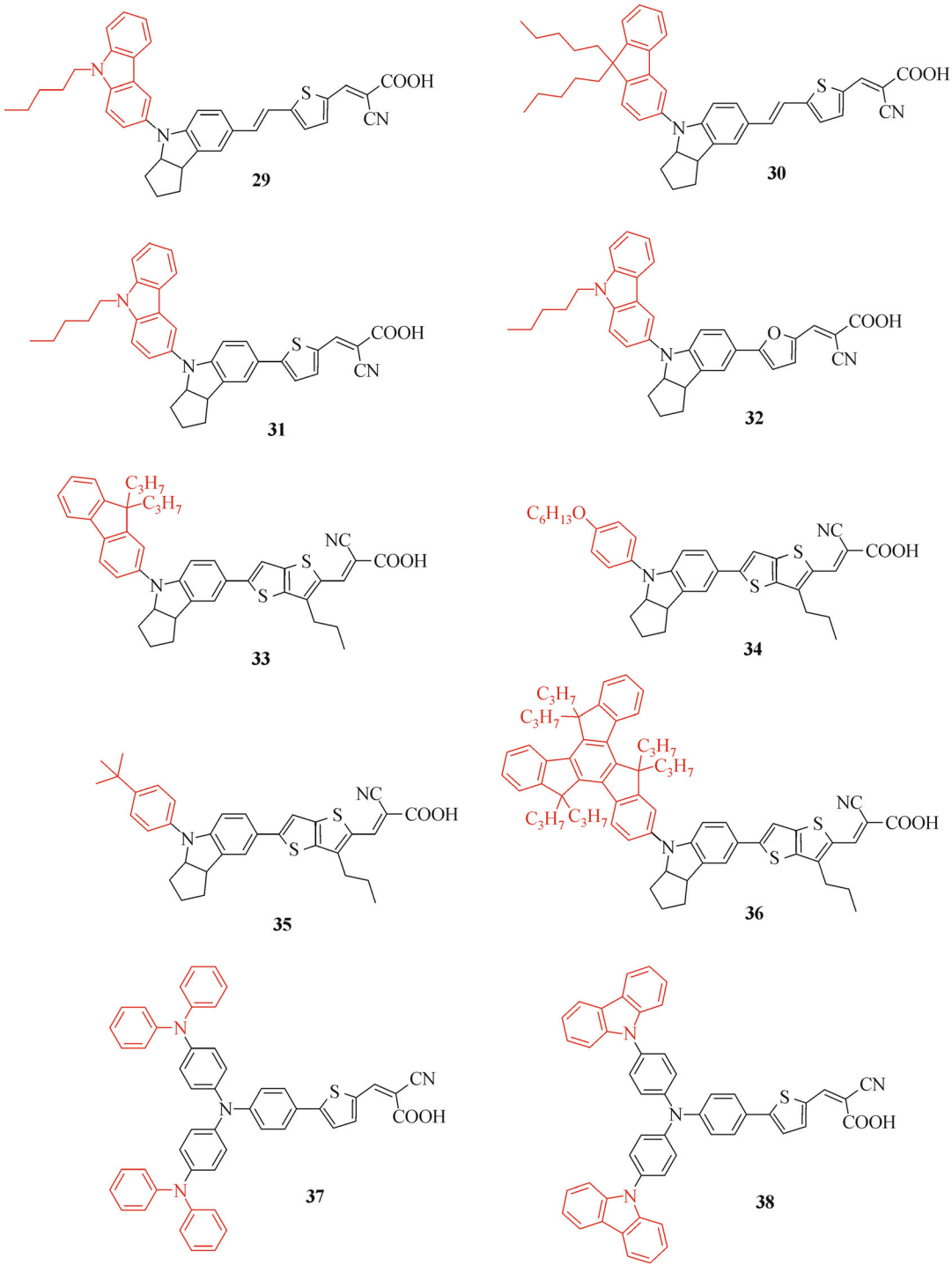

Scheme 3 Molecular structures of dyes **29**–**38**

However, this strategy is not always efficacious in every system. For example, our group showed two starburst dyes **37** and **38** with diphenylamine and carbazole as additional donor had almost the same device performance (PCE of 4.41% for dye **37** and PCE of 4.44% for dye **38**) with their D-π-A triphenylamine analog **19** (PCE of 4.32%) with the co-adsorption of 5 mM CDCA. And the possibility of getting mismatched energy levels also becomes one drawback of this strategy. However, we found the dyes **37** and **38** exhibited much better long-term stability in

DSSCs with quasi-solid-state electrolyte over 1200 h at full sunlight and at 50°C [43].

2.3 Expand donor part into π-bridge to broaden the spectral response and accelerate ICT progress

Ko's group investigated thoroughly on fluorene-substituted triarylamine dyes and their derivatives (Scheme 4). By changing the phenyl unit of **39** (PCE of 7.20%) that connected the donor and π-bridge into benzo[*b*]thiophene, benzo[*b*]furan and 4, 4-dimethyl-4*H*-indeno[1,2-*b*]thiophene, they got three new dyes **40** (PCE of 7.43%), **41** (PCE of 6.65%) and **42** (PCE of 8.2%), respectively [44–47]. Absorption spectra measured in ethanol solution showed that the absorption peak was largely red-shifted all the way from 436 to 480 nm (436 nm for **39**; 456 nm for **40**; 463 nm for **41** and 480 nm for **42**). Unfortunately the HOMO level of **41** reached only 0.6 V vs. NHE, which might render a low dye regeneration efficiency and diminish the J_{sc} and PCE. Frontier molecular orbitals of **39**, **40**, **41** and **42** showed quite good planarity of phenyl, benzo[*b*]thiophene, benzo[*b*]furan and 4,4-dimethyl-4*H*-indeno[1,2-*b*]thiophene with thiophene unit. In **35**, the dihedral angle between phenyl and thiophene was 20.5° [44]. Interesting finding was that the dihedral angle between the indenothiophene and the thienyl unit in **42** was only 1.6°. What's more, the cyanoacrylic acid group is also almost coplanar with thiophene, presenting extremely good planarity from 4,4-dimethyl-4*H*-indeno[1,2-*b*]thiophene to the acceptor. The calculations also showed the HOMO of **42** was delocalized over the whole π-conjugated system from the fluorenylamino unit to the cyanoacrylic group and the lowest unoccupied molecular orbital (LUMO) was delocalized through the 4, 4-dimethyl-4*H*-indeno[1,2-*b*]thiophene to cyanoacrylic unit, indicating a good HOMO-LUMO coupling [47]. This shows that the 4,4-dimethyl-4*H*-indeno[1,2-*b*]thiophene moiety already became a part of π-bridge favors the ICT process. The highest PCE of 8.2% was achieved by DSSCs based on **42** under AM 1.5 illumination.

Similar strategy was also applied to organic dyes **43** and **44**. The absorption peak bathochromically shifted by 10 nm and the molar extinction coefficient increased from 73800 to 85000 $M^{-1}\cdot cm^{-1}$ upon replacing the phenyl by benzo[*b*]thiophene. Time-dependent density functional theory (TD-DFT) calculations revealed that the dihedral angle between donor part and 3,6-dihexylthieno[3,2-*b*]thiophene-based π-bridge decrease from 51° (**43**) to 46.6° (**44**). The better planarity of molecular structure not only benefited the optical properties but also accelerated the ICT progress. The IPCE response of **44** was extended to 770 nm and highest IPCE of 93% was reached at 475 nm. The IPCEs were over 80% at the wavelength range of 400 to 640 nm. The broad IPCE spectra of DSSCs of **44** led to the high J_{sc} of 17.61 mA/cm^2. Excellent PCE of 9.1% was achieved by DSSC based on **44**. In the same condition, high PCE of 8.0% was obtained by DSSC based on **43** with J_{sc} = 15.7 mA/cm^2 [48].

A further extension of this strategy is to use donor units with good electron-donating ability and hole transporting property as π-bridges and attach them directly to the acceptor part. Thus these units not only act as part of the donor but also the π-bridge. The push and pull effect is reinforced and the charge transfer and separation between the electron donor and acceptor in the molecule become more effective, resulting in a good IPCE and high J_{sc}. One of the good examples is presented by Sun's group. They constructed three D-D-π-A dyes with different π-bridges such as thiophene (**47**), 3-hexylthiophene (**46**) and 3,4-ethyldioxythiophene (**45**) and compared them with their analog without the π-bridge (**48**). **45**, **46** and **47** all exhibited higher molar extinction coefficients and more red-shifted absorption peaks than that of **48**. However, the astonishing fact is that all of their IPCE were much lower than **48**'s over the spectral region of 380 – 600 nm. DSSC based on **48** displayed extremely good IPCE over 90% from 450 to 575 nm. In contract, the IPCE of other three dyes are all below 80%, except the highest IPCE of **45** reaching 80%. Even though **45**, **46** and **47** had much broader IPCE response ranges than **48**, the highest J_{sc} of 14.90 mA/cm^2 and the highest PCE of 7.5% were obtained by DSSC based on **48**, while PCEs of DSSCs based on **45**, **46** and **47** ranged from 6.1 to 6.4%, with the J_{sc}s ranging from 13.25 to 14.01 mA/cm^2 [49].

We also observed the similar phenomenon (Scheme 5). By comparing two sensitizers based on triphenylamine substituted *N*-annulated perylene with (**49**) and without (**50**) thiophene as π-bridge, we found that the absorption peak of **50** was largely red-shifted by 40 nm compared to that of **49**, which can be ascribed to the good co-planarity of triphenylamine and *N*-annulated perylene and better ICT process. The IPCEs of **50** were much higher than that of **49**. As for the device performance, DSSC sensitized with **50** showed a high PCE of 8.28% with J_{sc} = 16.50 mA/cm^2, V_{oc} = 0.734 V and *FF* = 0.684 in contrast to the PCE of 4.90% obtained by DSSC based on **49** with J_{sc} = 10.75 mA/cm^2, V_{oc} = 0.655 V and *FF* = 0.700 [50].

Fused thiophene groups usually afford good charge transport properties and have been used as good donors for organic photovoltaic (OPV) and organic field-effect transistor (OFET) materials [51]. Zhou and his coworkers investigated the effect of the tetrathienoacene position within the sensitizers on its photovoltaic performance. Interestingly when the tetrathienoacene was attached directly to the triphenylamine donor, the dyes (**51** and **53**) demonstrated higher IPCE than their counterparts (**52** and **54**) with thiophene spacer between triphenylamine and tetrathienoacene. The results of femtosecond time-resolved photoluminescence (FTR-PL) quenching experiment on dye-sensitized TiO_2 films showed the

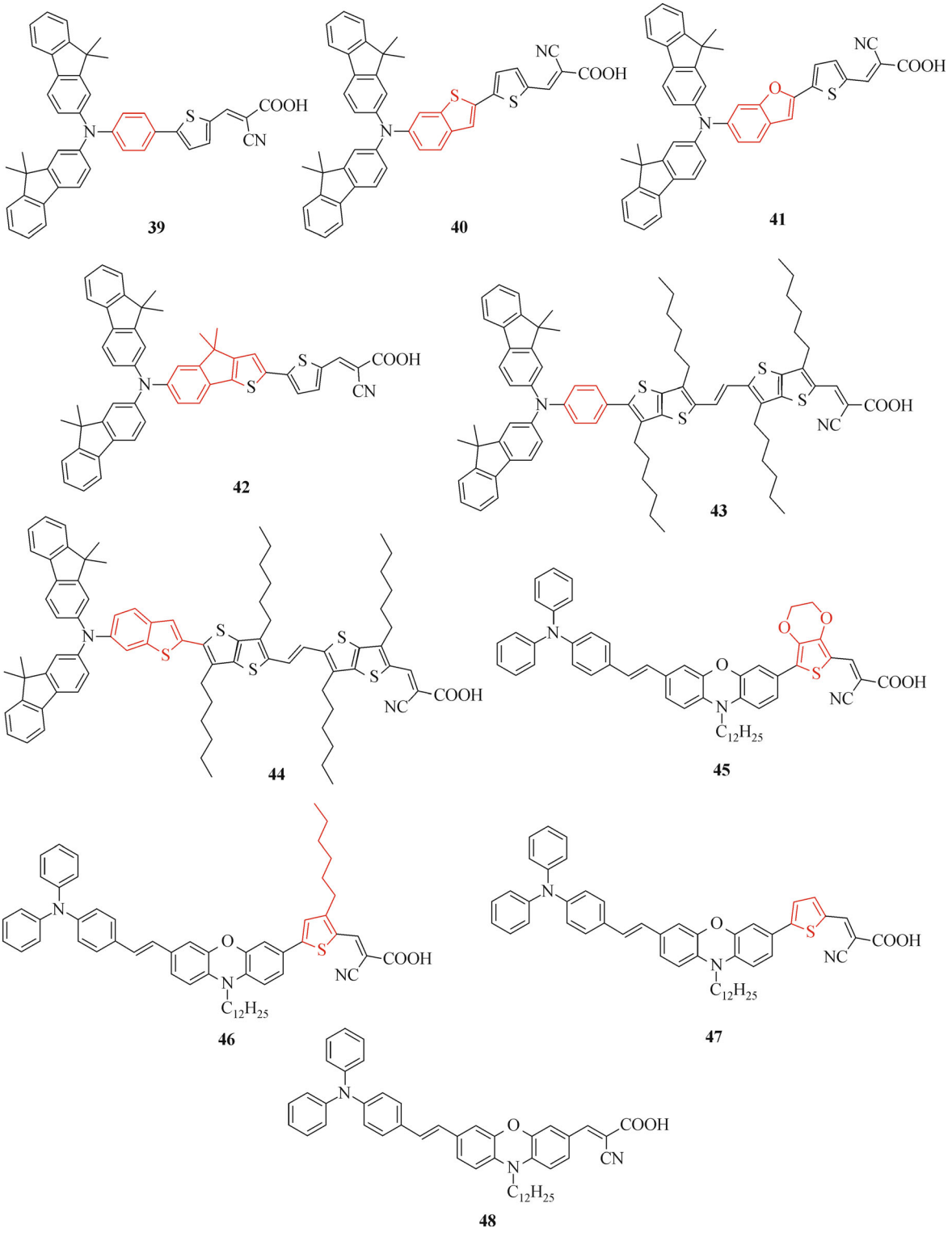

Scheme 4 Molecular structures of dyes **39**–**48**

sequence of electron injection efficiencies are **51** > **53** > **55** > **52**, offering indirect evidence for the benefits of extending the donor part into the π-bridge since tetrathienoacene can be regarded as donor and π-bridge. In addition, dye **53** gave the best IPCE spectra reaching 85% and an excellent PCE of 10.1% in DSSC with iodine electrolyte with J_{sc} = 16.5 mA/cm^2, V_{oc} = 0.833 V and *FF* = 0.737 [52].

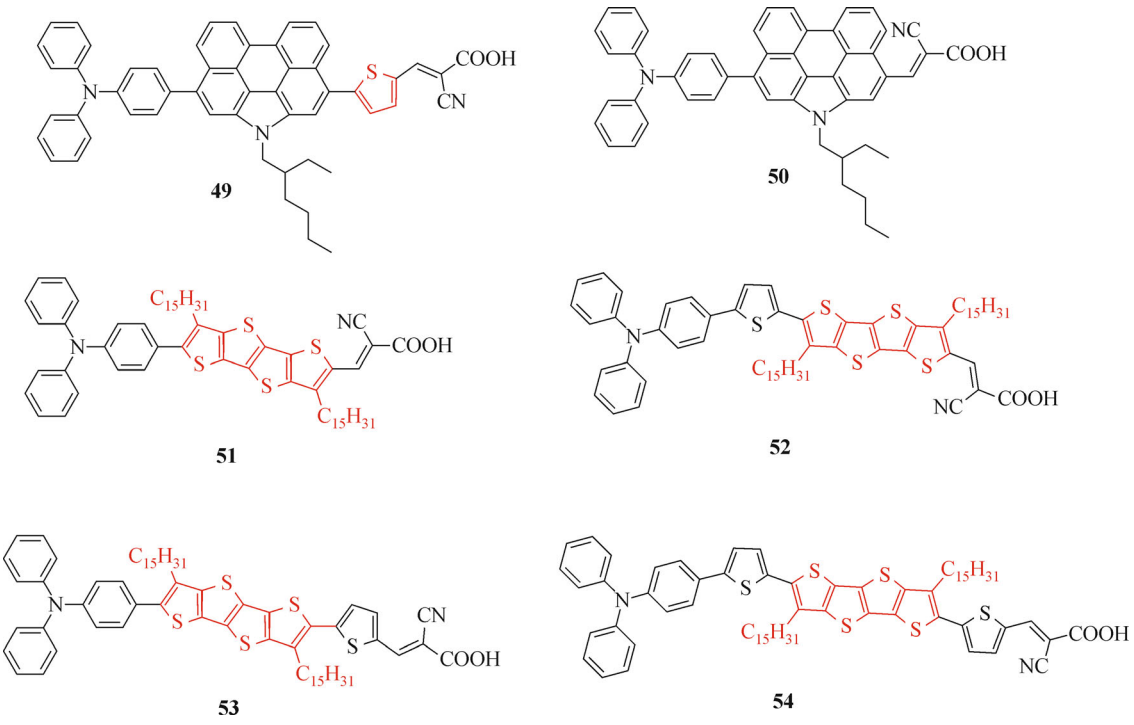

Scheme 5 Molecular structures of dyes **49**–**54**

2.4 Add blocking groups on donor unit to resist dye aggregation and charge recombination

Research showed that organic dyes are prone to form aggregates on the semiconductor surface, which can cause self-quenching of the excited state and increase the chance of charge recombination at the interface [53]. Adding blocking groups like long alkyl or alkyloxy groups has been proved to be an efficient approach to resist dye aggregation and charge recombination (Scheme 6). For example, in the research of bridged triphenylamine as donor done by Ko's group, the DFT/TD-DFT calculations of two **13** dye molecules adsorbed on adjacent Ti (IV) rows showed the formation of tight dye aggregates. They introduced $C_6H_{13}O$- and C_9H_{19}- onto the bridged triphenylamine to get dyes **55** and **56** respectively. Higher J_{sc}, V_{oc} and electron lifetime were all obtained in DSSCs based on **55** and **56** in the sequence of **56** > **55** > **13**, proving that the long chains on a donor unit can efficiently retard dye aggregation and charge recombination at the interface of TiO_2/dye/electrolyte, prolonging the electron lifetime and improving the photovoltaic performance. As a result, a high PCE of 8.71% with V_{oc} = 0.75 V was achieved by DSSC based on **56** and PCE of 8.28% with V_{oc} = 0.73 V was reached by DSSC based on **55** [33].

Sun's group and Hagfeldt's group extended the triphenylamine donor with *p*-dimethylamine and/or *p,o*-butoxy groups substituted phenyl groups to investigate the relationship between dye structure and overall efficiency of DSSCs. They first synthesized unsymmetric neutral metal-free sensitizer **58** with both *p*-dimethylamine and *p,o*-butoxy groups substituted phenyl groups, expecting to combine the properties from its parent dyes, **57** (only *p*-dimethylamine groups) and **59** (only *p,o*-butoxy groups). Because phenyl with *p*-dimethylamine has better electron-donating ability, **57** showed the broadest absorption band while **59** had the narrowest band. However, breaking the symmetry of the molecule led to orbital rearrangements and rendered the LUMO energy level of **58** much higher than that of **57** and **58** as well as the low molar extinction coefficient, which was only about half of **57**'s or **59**'s molar extinction coefficient. As for the device performance, J_{sc}s and V_{oc}s were both in the order of **59** > **58** > **57**, which probably because *p,o*-butoxy groups had much better effect on retard charge recombination and dye aggregation than *p*-dimethylamine. In the end, DSSC based on **59** yielded the highest PCE of 6.00%, thus showing the importance of using blocking chains to retard the charge recombination and dye aggregation to improve the overall solar cell efficiency [54].

Later, they used two long alkyl chains to replace the methyl groups on the tetrahydroquinoline part of **60** to get a new NIR dye **61**. Compared to **60**, there is a big increase on the molar extinction coefficient of **61**, reaching 88867 $M^{-1}\cdot cm^{-1}$. Also the DSSC based on **61** displayed an extremely high IPCE of 93% at 660 nm. The absorption peaks of these two dyes on TiO_2 films were red-shifted compared to their corresponding absorption peaks in solutions, which was in favor of light harvesting. This probably was due to J-aggregation since the deprotonation

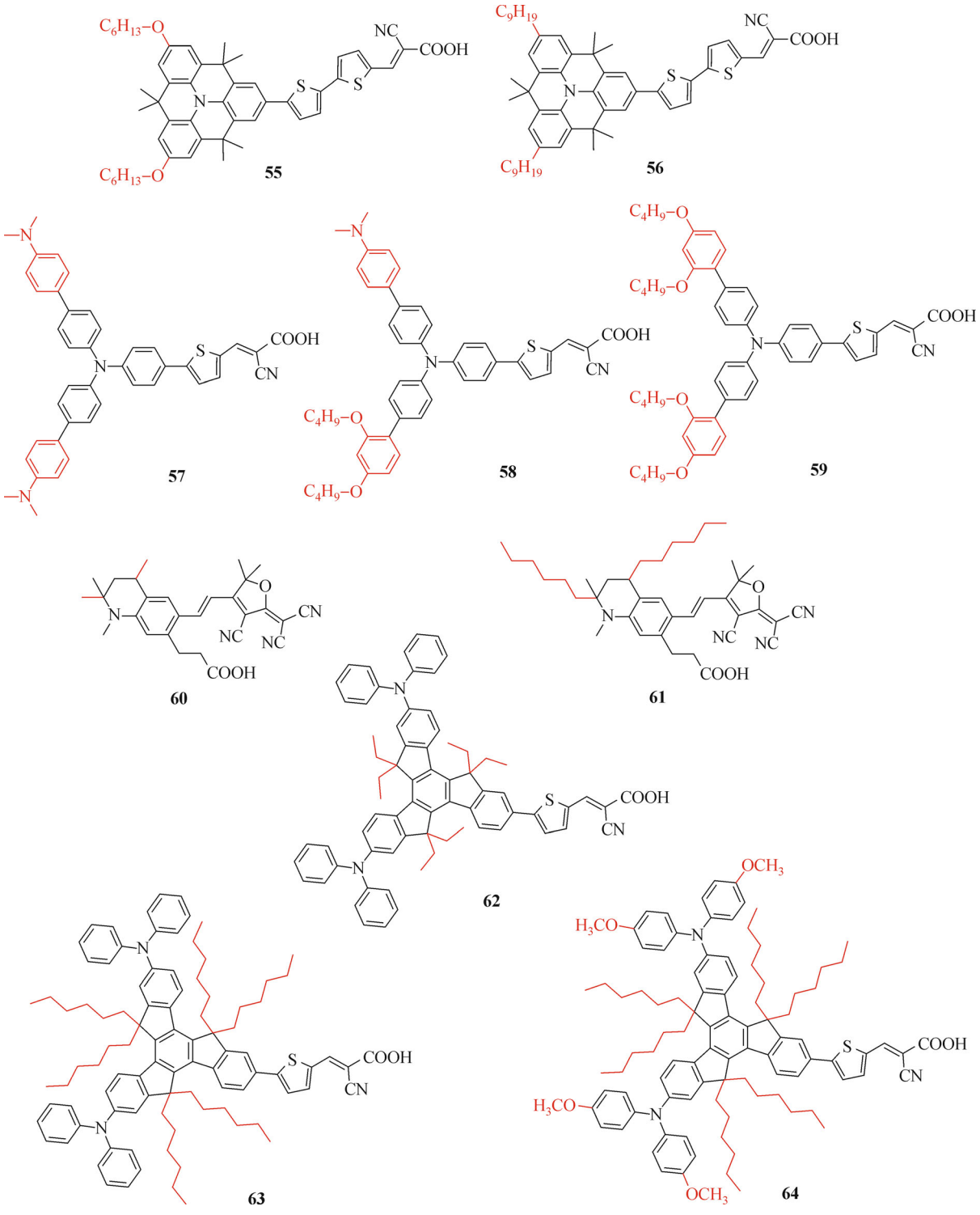

Scheme 6 Molecular structures of dyes **55**–**64**

of the dyes normally results in hypochromatic shift. Results also showed that the dye amount of **61** on the TiO_2 films was less than half of the amount of **60**, indicating **60** had a serious dye aggregation problem. The electrochemical impedance spectroscopy (EIS) showed the longer electron lifetime in DSSC based on **61**. As a result, DSSC based on **61** obtained PCE of 5.1% with J_{sc} = 13.35 mA/cm^2, V_{oc} = 0.519 V, FF = 0.73 while DSSCs based on **60** only gave PCE of 3.7%, J_{sc} = 11.76 mA/cm^2, V_{oc} = 0.464 V, FF = 0.674, proving the replacement with long

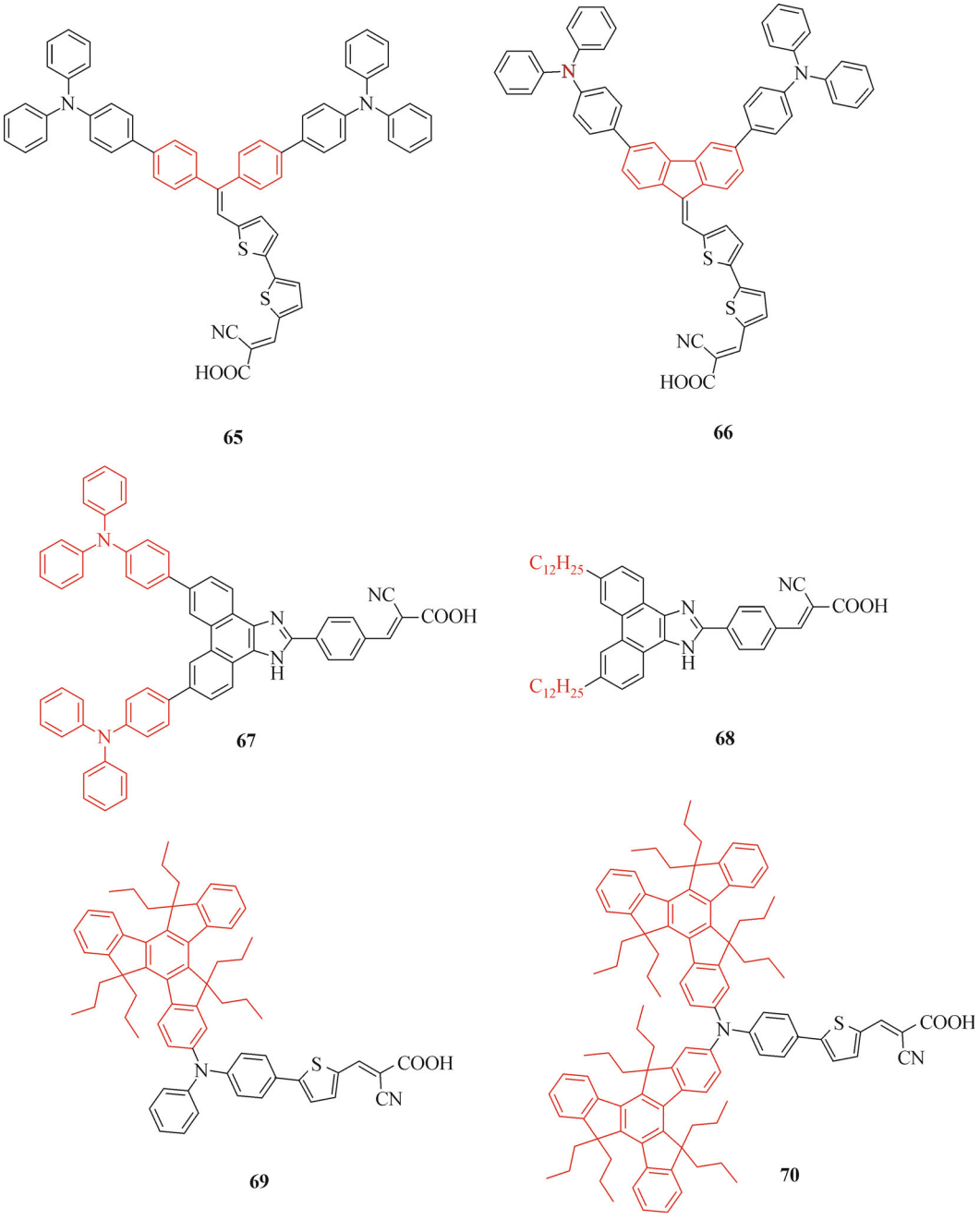

Scheme 7 Molecular structures of dyes **65**–**70**

alkyl chains can decrease the dye aggregation and charge recombination as well as improve the photovoltaic performance efficiently [55,56].

Our group synthesized a series of starburst truexene-based organic sensitizers (**62**, **63**, and **64**) with modifications of long hexyl chains on truexene part and methoxyl groups on diphenylamine segments. From **62** to **64**, the absorption peaks in CH_2Cl_2 were red-shifted from 406 to 430 nm and HOMO energy levels were shifted toward negative. The IPCEs of **62** and **63** were close to 90% but the IPCE of **64** was lower. This could be due to the low dye regeneration efficiency for lacking of driving force since the HOMO level of **64** was pushed too close to the redox potential of iodide/triiodide electrolyte. However, this did not affect the improvement of V_{oc} too much. By lengthening the ethyl groups to hexyl groups, the V_{oc} of DSSCs increased from 0.689 to 0.731 V. Then the V_{oc} was further improved to 0.752 V via adding methoxy groups on diphenylamine part, higher than 0.728 V obtained by DSSC based on **N719** in the same condition [57].

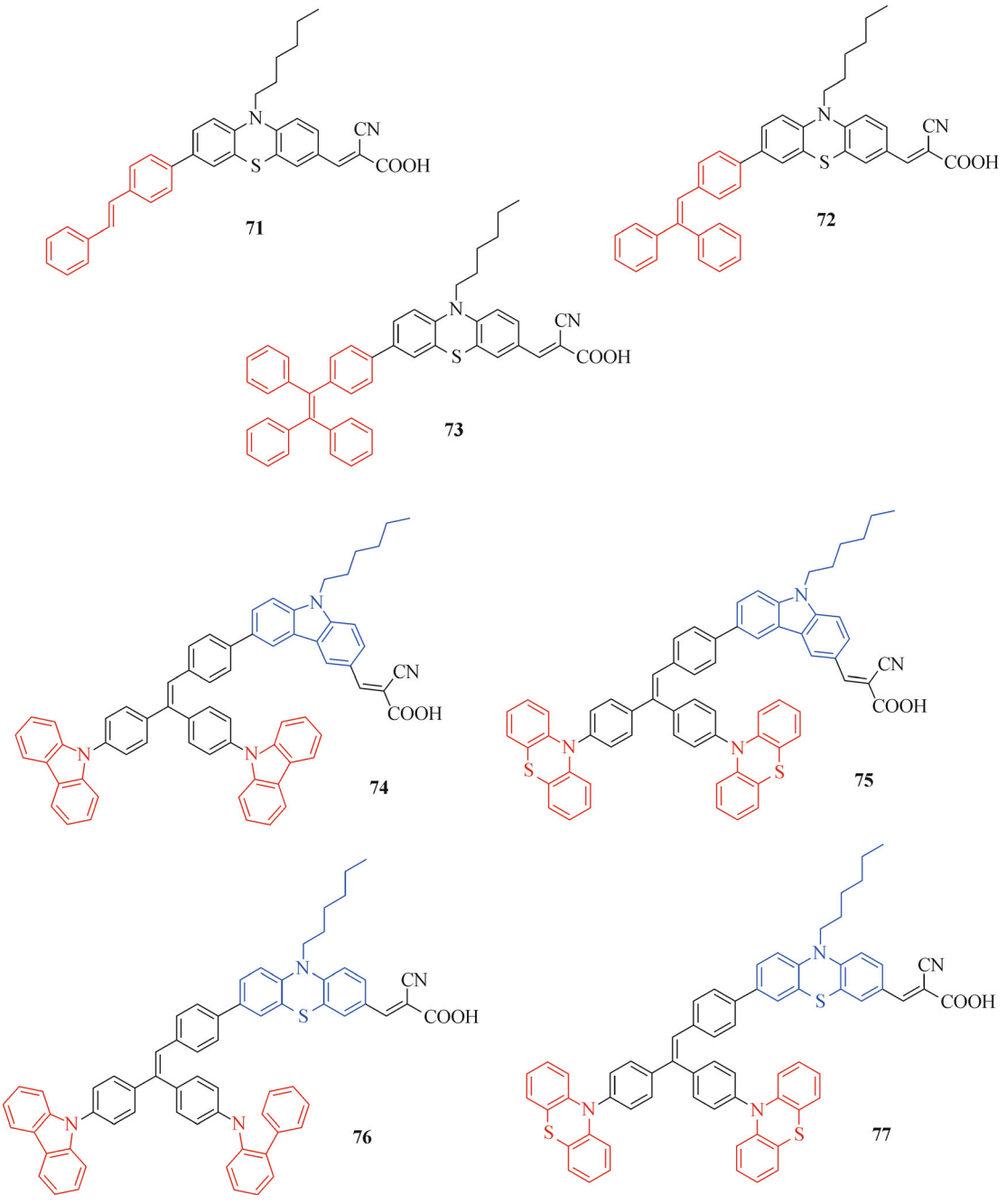

Scheme 8 Molecular structures of dyes **71**–**77**

2.5 Construct non-planar donor with large steric hindrance to resist dye aggregation and charge recombination

To avoid the consideration of the length and positions of blocking chains, using non-planar donor with large steric hindrance to resist the day aggregation and charge recombination is also seems to be an available choice (Scheme 7). To prove this, Han's group designed and synthesized two starburst organic dyes **65** and **66** with twisted and planar π-conjugation system. The absorption coefficient of **66** was higher than that of **65**, which can be ascribed to the wider and more planar π-conjugation system of **66**. They measured the maximum absorption wavelength of the dyes adsorbed on the surface of 2.3 μm-thick TiO_2 films with and without the co-adsorption of DCA and found that for **65**, the maximum absorption wavelength was 441 nm no matter if DCA was adsorbed while for **66**, the maximum absorption wavelength blue-shifted by 4 nm after co-adsorption with DCA, which can be attributed to the suppression of J-aggregates.

In the case of no DCA, the IPCE maximum of **65** based device reached about 80%, much higher than that of **66**, which is only about 50% despite of its high molar extinction coefficient. The **65**-based DSSC offered a PCE of 5.35% with J_{sc} = 10.359 mA/cm^2, V_{oc} = 0.715 V, FF = 0.722 while DSSC based on **66** only gave PCE of 3.20%, J_{sc} = 6.866 mA/cm^2, V_{oc} = 0.687 V, FF = 0.678. After co-sensitized with 20 mM DCA, the J_{sc} and PCE of DSSC based on **65** were slightly decreased whereas the J_{sc} and PCE of DSSC based on **66** were increased to 7.481 mA/cm^2 and 3.75%, respectively. Therefore, they came up with a conclusion that the twisted dye molecular structure can also efficiently suppress the dye aggregation and charge recombination [58].

Tsai et. al. compared the shielding effect of twisted D-D-π-A (**67**) and its corresponding D-π-A with long alkyl chains (**68**) in a 1*H*-phenanthro[9,10-*d*]imidazole-based system. They found that incorporation of triphenylamine groups at 1*H*-phenanthro[9,10-*d*]imidazole not only can retard charge recombination of the electrons, but also benefit from the enhancement of light-harvesting ability. In the end, DSSC based on **67** yield a better PCE of 4.68% than 4.01% of DSSC based on **68** even though it had higher V_{oc} [59].

Xue's group developed several truexene-based triphenylamine dyes. They found out that the large steric hindrance brought by truexene segments can effectively suppress dye aggregation and reach high V_{oc}. Taking **19** (PCE of 4.55%), **69** (PCE of 4.92%) and **70** (PCE of 5.23%) as examples, V_{oc}s of DSSCs based on **69** and **70** with no CDCA were 0.750 and 0.754 V, much higher than 0.690 V of **19**-sensitized DSSC. According to the absorption spectra measured in CH_2Cl_2 solution with the same dye concentration of 1.0×10^{-5} M, the bathochromic shifts of absorption peak and increase of molar extinction coefficients of **69** and **70** (65000 $M^{-1} \cdot cm^{-1}$ at 486 nm for **69**; 52000 $M^{-1} \cdot cm^{-1}$ at 498 nm for **70**) compared to **19** (28000 $M^{-1} \cdot cm^{-1}$ at 474 nm) can be mainly attribute to the stronger electron-donating ability of truexene, which are favorable for light harvesting. However, the large steric hindrance also reduced dye loading amount. For instance, the dye loading amount of **19** (1.25×10^{-7} mol/cm^2) on the TiO_2 surface is about 1.5 times of that of **69** dye (0.80×10^{-7} mol/cm^2), rendering the similar IPCE of **19** and **69**. Same case is also for **70**, the dye loading amount of **19** (1.8×10^{-7} mol/cm^2) is as twice as that of **70** (0.91×10^{-7} mol/cm^2). Therefore, no obvious improvement of J_{sc} was observed in DSSCs of **19** (9.7 mA/cm^2), **69** (9.8 mA/cm^2) and **70** (10.2 mA/cm^2), limiting the enhancement of PCE [60,61].

Chen and his colleagues worked on a series phenothiazine-based dyes (Scheme 8). They studied the difference of diphenylethylene (**71**), triphenylethylene (**72**), and tetraphenylethylene (**73**) substituted phenothiazine-based D-D-π-A dyes. The optical and electrochemical properties of these three dyes are almost the same, resulting in the similar IPCE spectra and J_{sc}s. However, big increments in V_{oc} were observed with the increasing size of polyphenyl-substituted ethylene. High V_{oc} of 0.804 V was reached by **73**-sensitized DSSC. The dark current and open-circuit voltage decay study suggested that more twisted donor structures of the dyes had an advantage in slowing down the electron recombination kinetics and lengthening the electron lifetime. Intensity modulated photovoltage spectroscopy (IMVS) and intensity modulated photocurrent spectroscopy (IMPS) revealed that the rigid tetraphenylethylene might pose a negative effect on the electron transport under increasing light intensity. With a twisted but a smaller steric hindrance effect on phenothiazine than tetraphenylethylene, triphenylethylene as the capping donor was more favorable in terms of charge transport and recombination suppression. With J_{sc} = 12.62 mA/cm^2, V_{oc} = 0.789 V and FF = 0.63, the highest PCE of 6.29% was obtained by DSSC based on **72** [62].

Similarly, they compared the effect of phenothiazine and carbazole as the capping donor and π-bridge in four triphenylethylene-based sensitizers. Results showed comparing with planar carbazole, phenothiazine is not only a good choice for donor with strong electron-donating ability, but also favorable for getting high V_{oc} because its nonplanar butterfly conformation can effectively retard molecular aggregation and dye aggregation. The highest PCE of 6.55% was produced by DSSCs based on **77** employing phenothiazine as capping donors and π-bridge with J_{sc} = 12.18 mA/cm^2, V_{oc} = 0.826 V and FF = 0.65. DSSCs based on **74**, **75** and **76** yielded the PCEs of 2.14%, 2.69% and 5.51%, respectively [63].

2.6 Introduce electron-withdrawing groups to fine tune the optical and electrochemical properties and accelerate the ICT process

By systematical study, our group found that introducing a strong electron-withdrawing group onto the donor is a very efficient method to essentially facilitate the electron transfer from the donor to the acceptor and modulate the absorption spectra, energy levels, photovoltaic performance as well as the photostability of sensitizers [64,65]. Many kinds of electron-withdrawing groups have been applied to organic sensitizers using this strategy, such as benzothiadiazole [66–74], benzotriazole [75–78], benzoxadiazole [79], quinoxaline [80–84], pyrido[3,4-*b*]pyrazine [85–87], [1,2,5]thiodiazolo[3,4-*c*]pyridine [88–90], thieno[3,4-*c*]pyrrole-4,6-dione [91,92], diketopyrrolopyrrole [93–98], and isoindigo units [99–101]. Some examples have been showed in Fig. 4.

For instance, by incorporating benzothiadiazole with indoline donor (Scheme 9), dye **79** showed a 27-nm bathochromic shift of the absorption band compared to its reference D-π-A dye **78** in CH_2Cl_2. DSSC based on **79** yielded a higher PCE of 8.15% with J_{sc} = 16.91 mA/cm^2, V_{oc} = 0.672 V and FF = 0.717 while 5.97% for DSSC

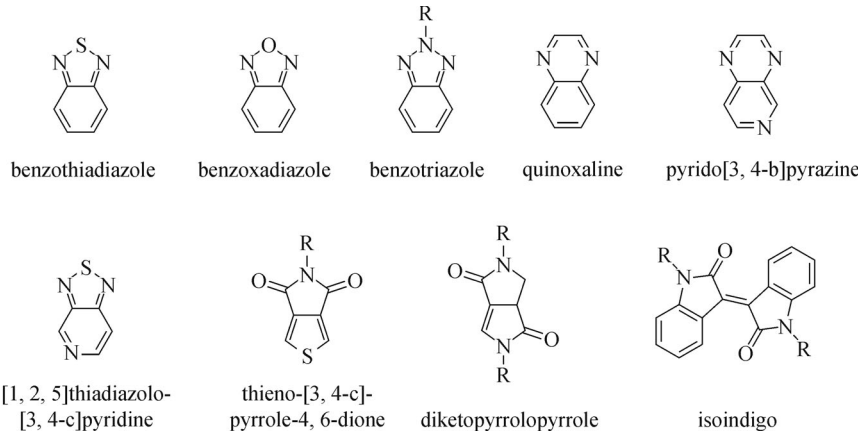

Fig. 4 Examples of electron-withdrawing groups used in organic sensitizers for DSSCs

based on **78** with J_{sc} = 13.77 mA/cm^2, V_{oc} = 0.615 V and FF = 0.705. The higher J_{sc} can be attributed to the much higher and boarder IPCE spectra of DSSC based on **79** than that of **78**. The results of stepped light-induced transient (SLIT) measurements and dipole moment calculations showed that the E_{CB} of TiO_2 can be upshifted by introducing benzothiadiazole in between the donor and π-bridge, thus improving V_{oc}. **79** also showed an excellent photostability, indicating the electron-withdrawing group can effectively stabilize indoline donor [73]. Different donors, triphenylamine (**80**), methoxyl substituted triphenylaime (**81**) and indoline (**82**) units, were also compared in benzothiadiazole-based system with CPDT as π-bridge. The sequence of electron-donating ability of the three donors is indoline > methoxyl substituted triphenylaime > triphenylamine. Interesting result of IPCE spectra was that even though the order of onset wavelength was in accordance with the electron-donating ability, the plateau of the IPCE spectrum of DSSC based on **81** was much lower than the others, only reaching 60%. Unfortunately this phenomenon was not explained in the paper. After all, DSSC based on **82** achieved the highest PCE of 10.08% with a high J_{sc} of 19.69 mA/cm^2 [74].

Introduction of electron-withdrawing groups also offers another approach for molecular modification. For example, **83** and **84** were designed and synthesized with methyl and octyl substituted benzotriazole groups, respectively. Results exhibited that the octyl chains posed a good effect on retarding the charge recombination and dye aggregation and increment of 0.1 V for V_{oc} was obtained under the same condition. PCEs of 6.74% and 8.02% were offered by DSSCs based on **83** and **84**, respectively [75]. Similarly, 2,3-bis(4-methoxyphenyl)quinoxaline and 2,3-bis(4-(octyloxy)phenyl)quinoxaline were also adopted as electron-withdrawing group attaching to indoline donor, providing dye **85** and **86**. The usage of long octyloxy chains successfully suppressed the charge recombination of electrons in TiO_2 conduction band to the electrolyte and dye aggregation, enhanced the electron lifetime and V_{oc} values. Without any co-adsorbent, DSSC based on **86** exhibited a high V_{oc} of 0.776 V and J_{sc} of 15.65 mA/cm^2, yielding a high overall DSSC efficiency of 8.50% under AM 1.5 illumination. PCE of 6.24% was given by DSSC based on **85** in the same condition with J_{sc} = 13.60 mA/cm^2 and V_{oc} of 0.685 V [80].

Our group designed and synthesized a series of triphenylamine-based sensitizers with pyrido[3,4-*b*]pyrazine (**87**) and 2,3-bis(4-methoxyphenyl)pyrido[3,4-*b*]pyrazine (**88** and **89**) as electron-withdrawing groups. Although barely changing the optical and electrochemical properties of the sensitizer, methoxyphenyl substitutions on the pyrido[3,4-*b*]pyrazine unit produced immediate effects of preventing dye-aggregation thus enhancing the J_{sc}, V_{oc} and PCE from 7.10 to 12.11 mA/cm^2, from 0.570 to 0.671 V and from 3.11% (**87**) to 6.14% (**88**), respectively. Further improvement was done by introducing octoxyl group on the triphenylamine unit (**89**). The maximum absorption wavelength of **89** was red-shifted to 524 nm and molar extinction coefficient was increased, contributing to the high J_{sc} of 13.56 mA/cm^2. The V_{oc} was also enhanced to 0.691 V, offering PCE of 7.12% [85].

Diketopyrrolopyrrole (DPP) has a strong electron-withdrawing capability which is promising to extend the absorption of dyes into NIR region. But the large π-conjugated system of DPP can cause a strong π-stacked aggregation on TiO_2 (Scheme 10). As a solution for that, we attached the butyl and 2-ethyl-hexyl chains in the middle of the DPP unit and obtained two dyes **90** and **91**. Both of them possessed broad spectral response and high molar extinction coefficients. Our results showed branched chains was better than straight chains in terms of reducing the dye aggregation and charge recombination for its bigger steric hindrance, resulting a high V_{oc}. As a result, DSSC based on **91** with indoline donor and 2-ethyl-hexyl substituted DPP unit achieved a high PCE of 7.43% with J_{sc} = 13.40 mA/cm^2, V_{oc} = 0.76 V, and FF = 0.73 while

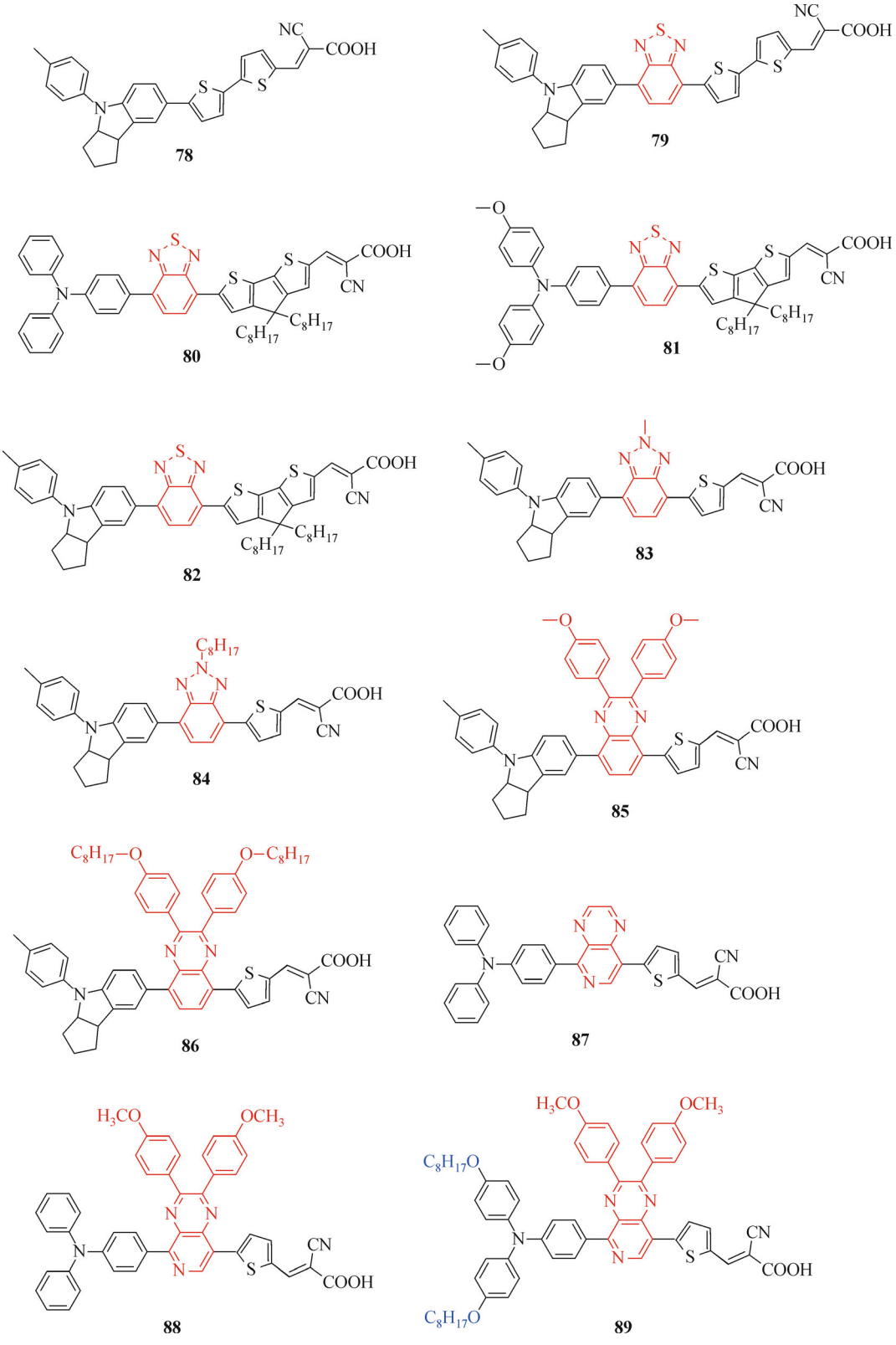

Scheme 9 Molecular structures of dyes **78**–**89**

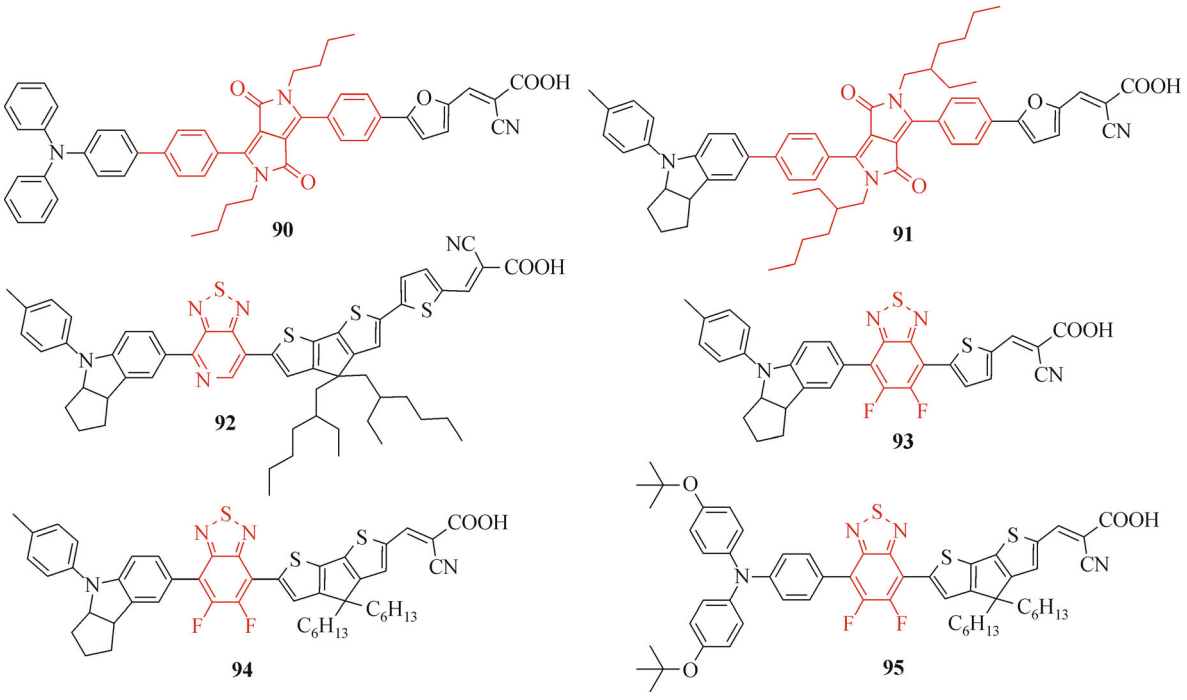

Scheme 10 Molecular structures of dyes **90**–**95**

DSSC based on **90** with triphenylamine donor and butyl substituted DPP unit yielded the PCE of 5.18% with J_{sc} = 11.05 mA/cm^2, V_{oc} of 0.69 V, and *FF* of 0.68. **91** also exhibited a good long-term stability [95].

Our group designed and synthesized a blue dye with the electron-withdrawing [1,2,5]thiadiazolo[3,4-*c*]pyridine unit attaching to the indoline donor. The absorption peak of **92** located at 593 nm with a molar extinction coefficient of 35800 $M^{-1}\cdot cm^{-1}$. With 2 mM CDCA as coadsorbent, the DSSC based on **92** showed a J_{sc} of 13.3 mA/cm^2, V_{oc} of 0.631 V and *FF* of 0.76, corresponding to the PCE of 6.4% [89].

Kang and his colleagues synthesized three organic dyes (**93**, **94** and **95**) with 5,6-difluoro-2,1,3-benzothiadiazole (DFBTD) as the electron-withdrawing group. Compared **93** with its 2,1,3-benzothiadiazole analog, they found two fluorine atoms on DFBTD unit can largely enhance the molar extinction coefficient but lead to a blue shift of the absorption band. By optimizing the π-bridge, strong absorption band with a red-shifted maximum absorption wavelength of 549 nm and a molar extinction coefficient of 55800 $M^{-1}\cdot cm^{-1}$ was obtained by **94**. Replacement of indoline with 4-(*tert*-butoxy)-*N*-(4-(*tert*-butoxy)phenyl)-*N*-phenylaniline led to a slightly blue shift of absorption peak and a decrease in molar extinction coefficient, resulting to a low J_{sc}. In the end, the highest PCE of 9.1% was yield by DSSC based on **94** with J_{sc} = 18.8 mA/cm^2, V_{oc} = 0.717 V, and *FF* = 0.673. In the same condition, PCEs of 7.4% and 6.6% were obtained by DSSCs based on **93** and **95**, respectively [102].

2.7 Other donors

Hundreds of organic sensitizers have been developed but the basic donor units are much less. New donor units need to be developed, especially strong donors for panchromatic sensitizers. Several new donor have been investigated (Scheme 11). For example, Franco et. al. designed and synthesized four organic sensitizers based on phenyl (**96** and **97**) or *tert*-butyl (**98**, and **99**) substituted *H*-pyran-4-ylidene as the donor for its proaromatic character. By adding hexyl chains on thiophene, the absorption peaks were successfully largely red-shifted by 24 and 33 nm for phenyl and *tert*-butyl substituted *H*-pyran-4-ylidene-based sensitizers, respectively, locating around 580 nm. However, the big drawback of this series was the low V_{oc} which were sacrificed for the broader spectrum response. The highest PCE of 5.37% was obtained by DSSC based on **99** with PCE of 6.9% for **N719** based DSSC as reference [103].

Some novel fused aromatic hetercyclic groups with long alkyl chains also have been developed as the donor of sensitizers for DSSCs. For example, Hara's group designed and synthesized two dyes based on 5,11-dioctylindolo[3,2-*b*]carbazole (**100** and **101**). Their absorption peaks were at about 500 nm and showed good IPCE. Under AM 1.5G irradiation, DSSC based on **100** gave a J_{sc} of 15.4 mA/cm^2 and V_{oc} of 0.71 V, yielding PCE of 7.3% while PCE of 6.7% for DSSC based on **101** with J_{sc} = 15.5 mA/cm^2 and V_{oc} = 0.70 V [104]. Paramasivam et. al. worked on benzocarbazole-based

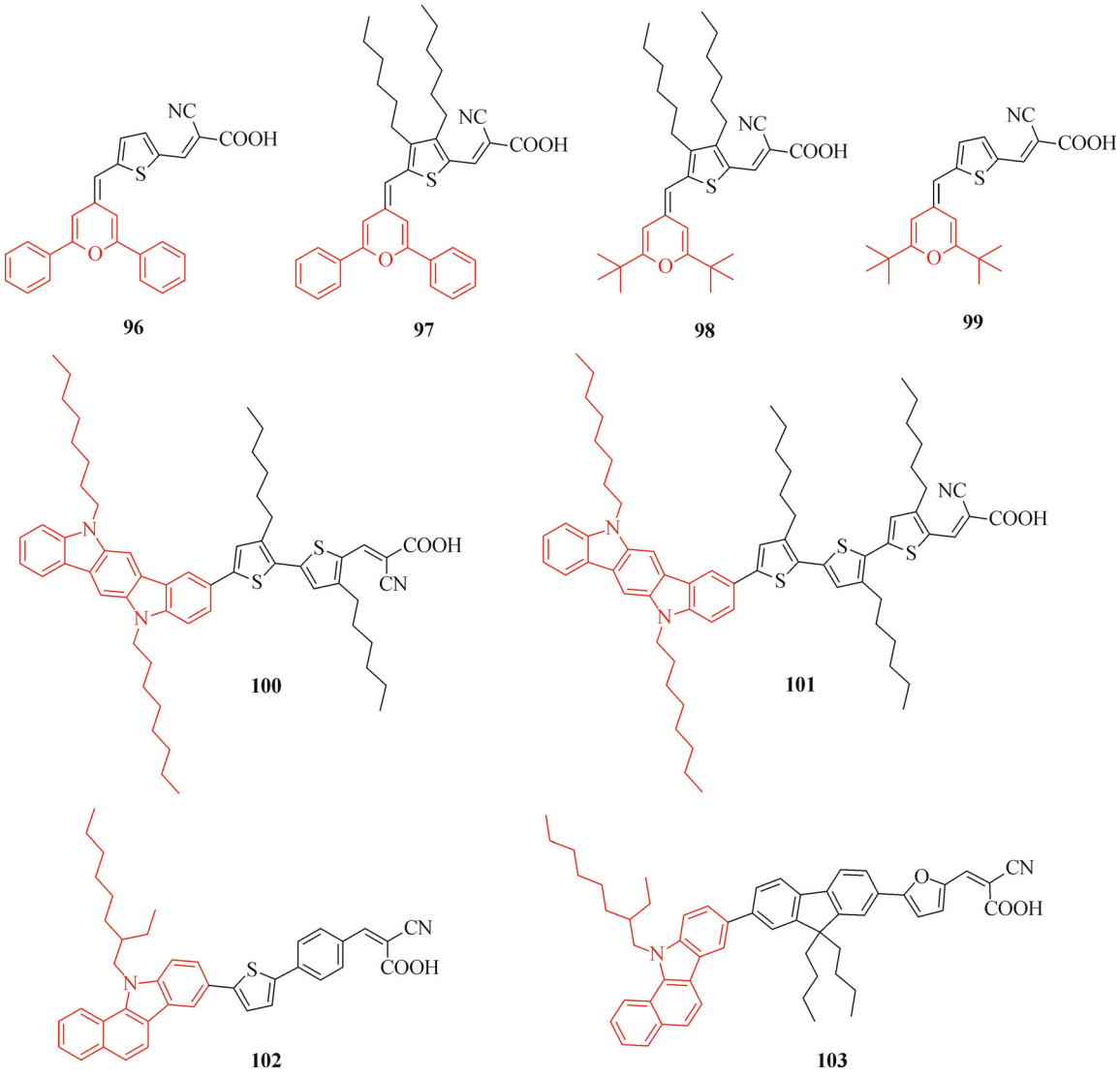

Scheme 11 Molecular structures of dyes **96**–**103**

sensitizers since benzocarbazole has a good hole transporting property and thermal stability. Taking dyes **102** and **103** for example, they had high molar extinction coefficients of 50623 and 60782 $M^{-1}\cdot cm^{-1}$ at 427 and 434 nm, respectively. Large bathochromic shifts (55 nm for **102** and 34 nm for **103**) were observed after the dyes absorbed onto the surface of mesoporous TiO_2 layer, which can be ascribed to the J-aggregation. With an iodide electrolyte, DSSC based on **102** afforded a J_{sc} of 10.18 mA/cm^2 and V_{oc} of 0.733 V, yielding PCE of 5.74% under AM 1.5G illumination while **103** sensitized DSSC gave PCE of 4.63% under the same condition [105].

Wu et. al. introduced cyclic thiourea/urea groups into triphenylamine donor (Scheme 12). They considered that the cyclic thiourea/urea group containing sulfur/oxygen and nitrogen atoms with lone pair electrons may pose a positive effect on the electron-donating ability and delocalizing the positive charges and the introduction of long alkyl chains can retard the charge recombination and improve the open circuit voltage. Dye **105** showed slightly weaker light harvesting capability than its thiourea analog **106**. **106** also did not have much more advantages compared to **104** that had no π-bridge. After modification of π-bridge with two thiophene units, **107** exhibited the red-shifted absorption peak at 443 nm in CH_2Cl_2 solution and IPCE over 70% in the wavelength of 400–600 nm in DSSCs, affording the highest J_{sc} of 14.8 mA/cm^2. With V_{oc} of 0.749 V and *FF* of 0.659, DSSC based on **107** yielded the highest PCE of 7.42%. The others gave PCEs of 4.94%, 4.73% and 5.33% for **104**, **105** and **106** respectively [106].

Grätzel's group reported a series of novel organic sensitizers with ullazine as donor. Ullazine is a planar π-system with an aromatic 14 π-electron annulene resonance structure. They connected the acceptor at the 4-, 5-, or 6-positions of the ullazine core and found that only acceptor

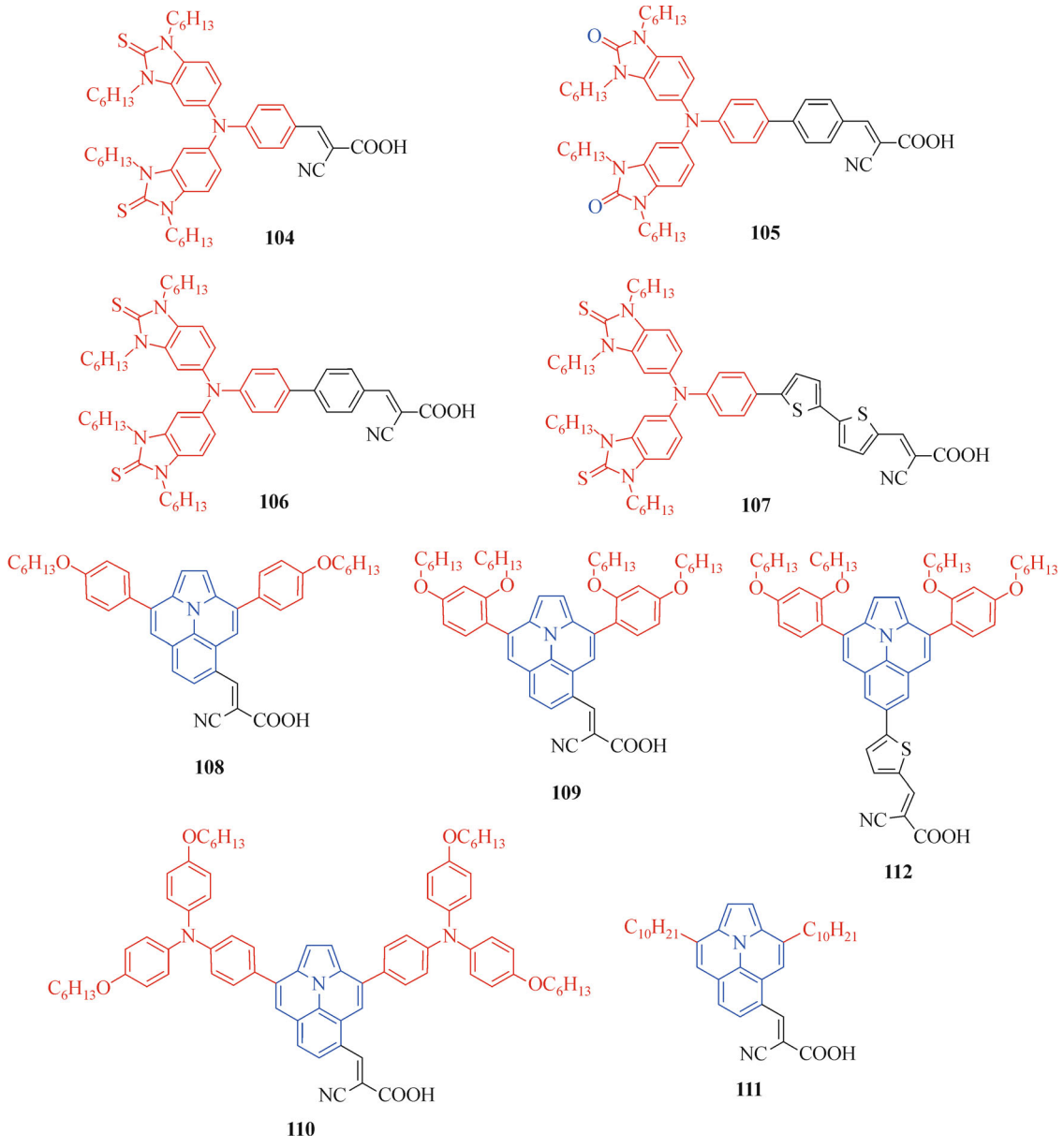

Scheme 12 Molecular structures of dyes **104**–**112**

at 5-position gave strong and red-shifted ICT band which was suitable for the sensitizers of DSSCs. With the thiophene π-bridge connecting to the 6-position of ullazine, the main absorption peak of **112** hypochromatically shifted by 189 nm and the shoulder peak at 540 nm almost disappeared, only giving a low molar extinction of 1600 $M^{-1}\cdot cm^{-1}$. DSSC based on **112** also gave poor PCE of 1.7%. On the contrary, among those dyes with acceptor at the 5-position of ullazine core, dyes **108**, **109** and **110** showed a broad absorption range with the maximum absorption wavelength of 582, 598 and 598, respectively. The one with only decyl substituted ullazine core as donor also afford an ICT band at 531 nm. Broad IPCE spectra of **108**, **109**, **110** and **111** sensitized DSSCs were observed with the onset wavelength exceeding 700 nm. The highest PCE of 8.4% was achieved by DSSC based on **108** with J_{sc} = 15.4 mA/cm^2, V_{oc} = 0.730 V and FF = 0.75 in conjunction with iodide/triiodide redox electrolyte under AM 1.5G illumination. In the same condition, **109**-, **110**- and **111**-sensitized solar cells provided PCEs of 6.7%, 6.7% and 5.2%, respectively [107].

In a nut shell, all these donor design and modification strategies of metal-free sensitizers aim at enhancing the photocurrent and photovoltage thus yielding a high overall solar cell efficiency. Recently, Joly and his coworkers developed several triphenylamine based sensitizers which achieved the new record PCE exceeding 10% with iodine electrolyte. Here we take four of them as examples since

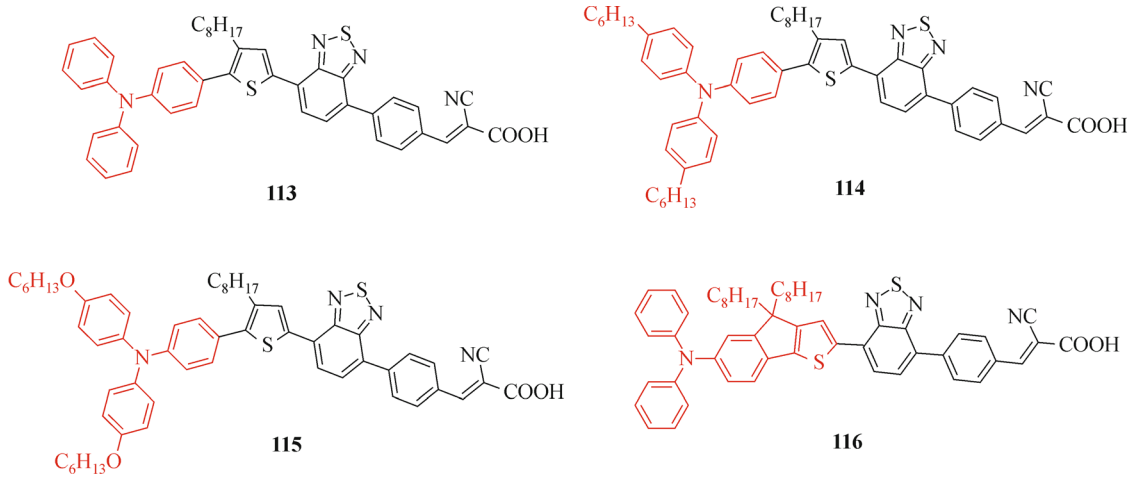

Scheme 13 Molecular structures of dyes **113**–**116**

they used the strategies such as adding blocking chains, extending the donor part to π-bridge and connecting electron-withdrawing group with donor (Scheme 13). We can see compared to **113**, the absorption peak red-shifted by 6 and 14 nm by adding the hexyl and hexyloxy groups, respectively. While bathochromic shift of 38 nm was shown via extending the donor by the fusion between the triphenylamine and the thiophene unit. In conjugation with iodine electrolyte consisting of 0.5 M 1-butyl-3-methyl-imidazolium iodide (BMII), 0.1 M LiI, 0.05 M I_2 and 0.5 M *tert*-butyl-pyridine in acetonitrile, all of the four dyes exhibited high IPCE over 80% in DSSC, especially IPCE of DSSCs based on **113** and **116** were close to 100%, offering high J_{sc} of 16.76 – 18.82 mA/cm^2. The V_{oc}s were almost the same for devices based on these dyes. After device optimization, DSSCs based on **113**, **114**, **115** and **116** yielded excellent PCEs of 10.20%, 9.67%, 10.11% and 9.69%, respectively [108].

3 Strategies for donor design and modification in DSSCs with cobalt electrolyte

It has been pointed out that the large potential loss in DSSC system is one of the reasons that limit its PCE due to the over-potentials required by electron injection and dye regeneration processes [109]. The standard potential of I^-/I_3^- redox couple of 0.35 V vs. NHE results in a high overpotential for the dye-regeneration reaction and a big loss in potential, diminishing the V_{oc} and PCE, let alone its competitive light absorption and strong corrosiveness toward most of metals. Therefore, many alternative redox electrolytes have been developed [14,110–114]. Among them, cobalt complexes attracted most of researchers for its tunable redox potential, negligible light absorption and remarkable performance in DSSCs [114–117]. However, the thickness of TiO_2 films is limited because of the mass transport and charge recombination problems due to the larger size, heavier mass and lower diffusion coefficient of cobalt complexes [118] Therefore, organic sensitizers with high molar extinction coefficients are desirable to DSSCs with cobalt electrolyte.

In 2010, Hagfeldt's group first reported DSSCs with cobalt electrolyte surpassing the PCE of their counterpart with iodide electrolyte using **59** with bulky triphenylamine donor and long alkyloxy chains. Four different cobalt complex-based redox couples: cobalt(III/II) tris(2,2′-bipyridine) ($[Co(bpy)_3]^{3+/2+}$), cobalt(III/II) tris(4,4′-dimethyl-2,2′-bipyridine) ($[Co(dmb)_3]^{3+/2+}$), cobalt(III/II) tris(4,4′-ditert-butyl-2,2′-bipyridine) ($[Co(dtb)_3]^{3+/2+}$), and cobalt (III/II) tris(1,10-phenanthroline) ($[Co(phen)_3]^{3+/2+}$) were compared in DSSCs based on **57** and **59**. They found that recombination can be retarded more effectively by introducing insulating alkyl/alkyloxy chains on the dye rather than on the cobalt redox couples. The blocking chains on the ligands of cobalt complexes cannot only slow down the diffusion of the redox couples but also positively shift the redox potential, imperilling the J_{sc}, V_{oc} and thus PCE of the device. In the end, DSSCs based on **59** with *o*, *p*-dibutoxyphenyl substituted triphenylamine donor achieved the highest PCE of 6.7% with a high V_{oc} of 0.92 V and J_{sc} of 10.7 mA/cm^2 under AM1.5G illumination using 0.5 M $Co(bpy)_3(PF_6)_2$, 0.1 M $Co(bpy)_3(PF_6)_3$, 0.5 M TBP, and 0.1 M $LiClO_4$ in acetonitrile as redox electrolyte whereas PCE of 5.5% by its counterpart with iodine electrolyte in the same condition [7].

Specified investigation was carried out in our group and Grätzel's group on the donor size and their influence on DSSC performance with cobalt electrolyte and iodine electrolyte (Scheme 14). We constructed three organic sensitizers with different indoline donor size and electron-withdrawing quinoxaline. The sequence of the donor size is **117** < **118** < **119**. Through the comparison in DSSCs with cobalt and iodide electrolyte with platinum counter

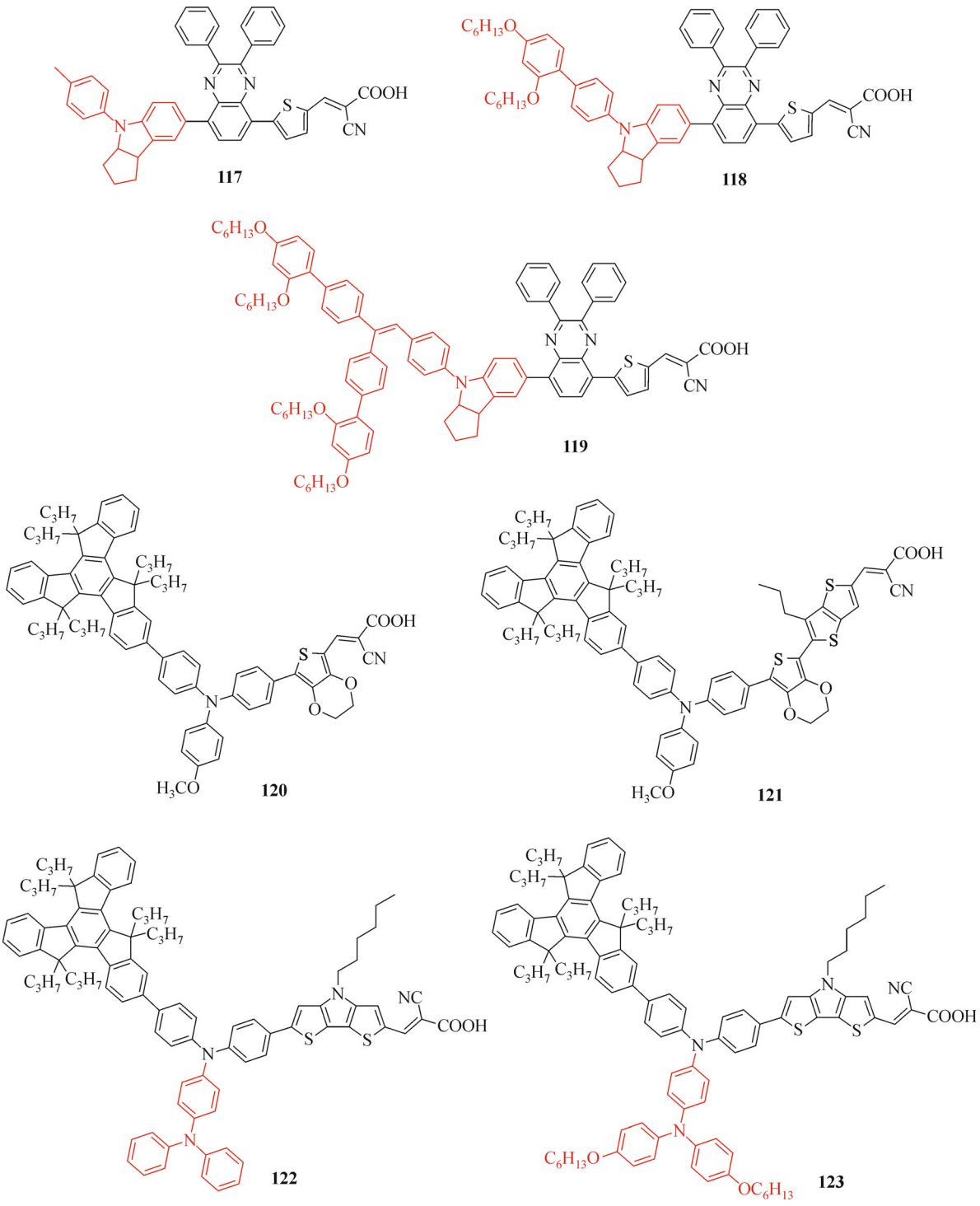

Scheme 14 Molecular structures of dyes **117**–**123**

electrode, we found the three dyes showed opposite trend (PCE: **117** > **118** > **119** in iodide electrolyte in contrast with **119** > **118** > **117** in cobalt electrolyte), indicating the electron recombination process was efficiently impeded because of the shielding effect of bulky donor with long alkyloxy chains in cobalt electrolyte whereas retarded the dye regeneration in iodide electrolyte. Since platinum is not a good catalyst for cobalt redox couples, graphene nanoplatelets (GNP) was used as counter electrode to further improve the performance of DSSCs with cobalt electrolyte. The device performance was the same and **119** sensitized DSSC obtained PCE of 9.60%. Further

optimization was carried out using Au + GNP as the counter electrode and 10.65% PCE was achieved with 0.22 M $Co(bpy)_3[B(CN)_4]_2$, 0.06 M $Co(bpy)_3[B(CN)_4]_3$, 0.1 M $LiClO_4$, and 0.5 M TBP in acetonitrile as redox electrolyte [119].

Therefore, the long blocking chains are necessary for good performed DSSCs employing cobalt electrolyte. The strategies of 2.2 – 2.7 are also valid for developing organic sensitizers for DSSCs with cobalt electrolyte. For example, truexene-based organic sensitizers are suitable for DSSC with cobalt electrolyte for its strong electron-donating ability and large steric hindrance with long alkyl chains. Xue's group works on this types of sensitizers by combining with triphenylamine unit to construct high performance D-D-π-A dyes, such as **120** and **121**. DSSC based on **120** showed PCE of 7.2% with J_{sc} = 12.0 mA/cm^2 and V_{oc} of 0.830 V in conjugation with $[Co(phen)_3]^{3+/2+}$-based electrolyte. V_{oc} of 0.900 V, J_{sc} of 11.9 mA/cm^2, and PCE of 7.6%, were produced by DSSCs based on **121** with 0.25 M $[Co(II)(phen)_3](PF_6)_2$, 0.05 M $[Co(III)(phen)_3](PF_6)_3$, 0.8 M TBP and 0.1 M LiTFSI (TFSI = bis (trifluoromethanesulfonyl)imide) in acetonitrile as redox electrolyte [120,121]. Later, they introduced diphenylamine (**122**) and hexyloxy subsitituted diphenylamine (**123**). Interestingly, the photovoltaic performance of DSSC based on **123** was inferior to that of **122** although it had a stronger light harvesting ability. Lacking of driving force for dye regeneration might be responsible for the lower J_{sc} of DSSC based on **123**. IMVS measurements also showed that the electron lifetime of the **123** sensitized DSCs was shorter than that of the **122**, resulting the lower V_{oc}. DSSC based on **122** exhibited J_{sc} of 14.32 mA/cm^2, V_{oc} of 0.907 V and *FF* of 0.68, corresponding to a high PCE of 8.83% with $[Co(phen)_3]^{3+/2+}$-based electrolyte whereas PCE of 7.81% for DSSC with **123** [122].

Consist of the bulky donor of **59**, CPDT as π-bridge and cyanoacetic acid as acceptor and anchor (Scheme 15), **124** has exhibited a good device performance in DSSC with cobalt electrolyte, offering PCE of 8.8% in the first report [123]. Later, with the usage of porous poly(3,4-ethylenedioxythiophene) (PEDOT) counter electrodes, DSSCs with **124** achieved PCE of 10.3% with $[Co(bpy)_3]^{3+/2+}$ electrolyte [124]. Many sensitizers based on **124** has been synthesized and applied to DSSC with cobalt electrolyte. For example, **125** was proposed as an analog of **124** with fluorene-substituted triarylamine donor attached with hexyloxy chains. It showed a stronger electron-donating property and slightly better device performance of 10.3% with J_{sc} = 16.2 mA/cm^2 and V_{oc} of 0.840 V whereas PCE of 9.8% for DSSCs based on **124** in the same condition [125]. Later, two analogs of **124** and **125** by replacing the CPDT unit with the dithieno[3,2-b:2′,3′-d]pyrrole π-bridge as DTP were also applied successfully to DSSCs with cobalt electrolyte, yielding PCE of 8.86% (**126**) and 8.72% (**127**), respectively [126].

Our group compared the differences between triphenylamine- and indoline-based bulky donors in two dyes with electron-withdrawing 2,3-diphenylpyrido[3,4-*b*]pyrazine group. The absorption peak of **129** was red-shifted by 16 nm compared to **130** due to the stronger electron-donating property of indoline. With the assistant of density functional theory calculations, we found the biphenyl branch at the *cis*-position of *N*-phenylindoline and the indoline core had very limited electronic contribution to the donor, which probably acted as an insulating blocking group to inhibit the dye aggregation and charge recombination at the interface of TiO_2/dye/electrolyte. The measurement results also showed the charge recombination in DSSCs based on **129** was much less than that of **130**, probably because of the bigger donor size and the shielding effect of the donor of **129**. In DSSCs with $[Co(bpy)_3]^{3+/2+}$ redox electrolyte, **129** presented a higher performance of 8.57% with J_{sc} = 16.08 mA/cm^2 and V_{oc} = 0.802 V while **130** gave PCE of 7.74%, J_{sc} = 15.35 mA/cm^2 and V_{oc} = 0.790 V under standard AM 1.5 G simulated sunlight [127]. Another bulky triphenylamine sensitizer **128** was investigated with $[Co(bpy)_3]^{3+/2+}$ redox electrolyte containing stacked graphene platelet nanofibers (SGNF). With 0.22 M $[Co(II)(bpy)_3](TFSI)_2$, 0.06 M $[Co(III)(bpy)_3](TFSI)_3$, 0.1 M $LiClO_4$, 0.5 M TBP and 0.2 mg/mL SGNF in acetonitrile as electrolyte, DSSC based on **128** obtained the highest PCE of 9.81% with J_{sc} = 16.75 mA/cm^2 and V_{oc} = 0.830 V [128].

Grätzel's group reported four blue-colored diketopyrrolopyrrole (DPP)-based sensitizers **131**, **132**, **133** and **134** with 4-(hexyloxy)-*N*-(4-(hexyloxy)phenyl)-*N*-phenylaniline, 4-(*p*-tolyl)-1,2,3,3a,4,8b-hexahydrocyclopenta[*b*]indole,4-(2',4'-bis(hexyloxy)-[1,1'-biphenyl]-4-yl)-1,2,3,3a,4,8b-hexa-hydrocyclopenta[*b*]indole and 4-(4-(2,2-bis(2',4'-bis(hexyloxy)-[1,1'-biphenyl]-4-yl)vinyl)phenyl)-1,2,3,3a,4,8b-hexahydrocyclopenta[*b*]indole as donor (Scheme 16). Indoline based sensitizer **132** (57100 $M^{-1}\cdot cm^{-1}$ at 596 nm), **133** (62400 $M^{-1}\cdot cm^{-1}$ at 600 nm) and **134** (69000 $M^{-1}\cdot cm^{-1}$ at 602 nm) had more advantages in light-harvesting ability then triphenylamine-based sensitizer **131** (55700 $M^{-1}\cdot cm^{-1}$ at 587 nm). With the expansion of indoline donor, the molar extinction coefficient increased and absorption peak slowly red-shifted. High IPCE was obtained at the range of 400 – 700 nm. **132** got the lowest V_{oc} for lacking of shielding protection from the charge recombination at the interface of TiO_2/dye/electrolyte. With the corporation of cobalt electrolyte, DSSCs based on **131**, **132**, **133** and **134** yielded high PCE of 8.97%, 8.23%, 9.81% and 10.1%, respectively [129].

Recently, Wang's group extended the π-conjugation system of *N*-annulated indenoperylene donor of **135** fixed the adjacent phenyl group with cyclopentadiene. The novel dye **136** possessed a red-shifted absorption band and much higher molar extinction coefficient than **135** contributing to

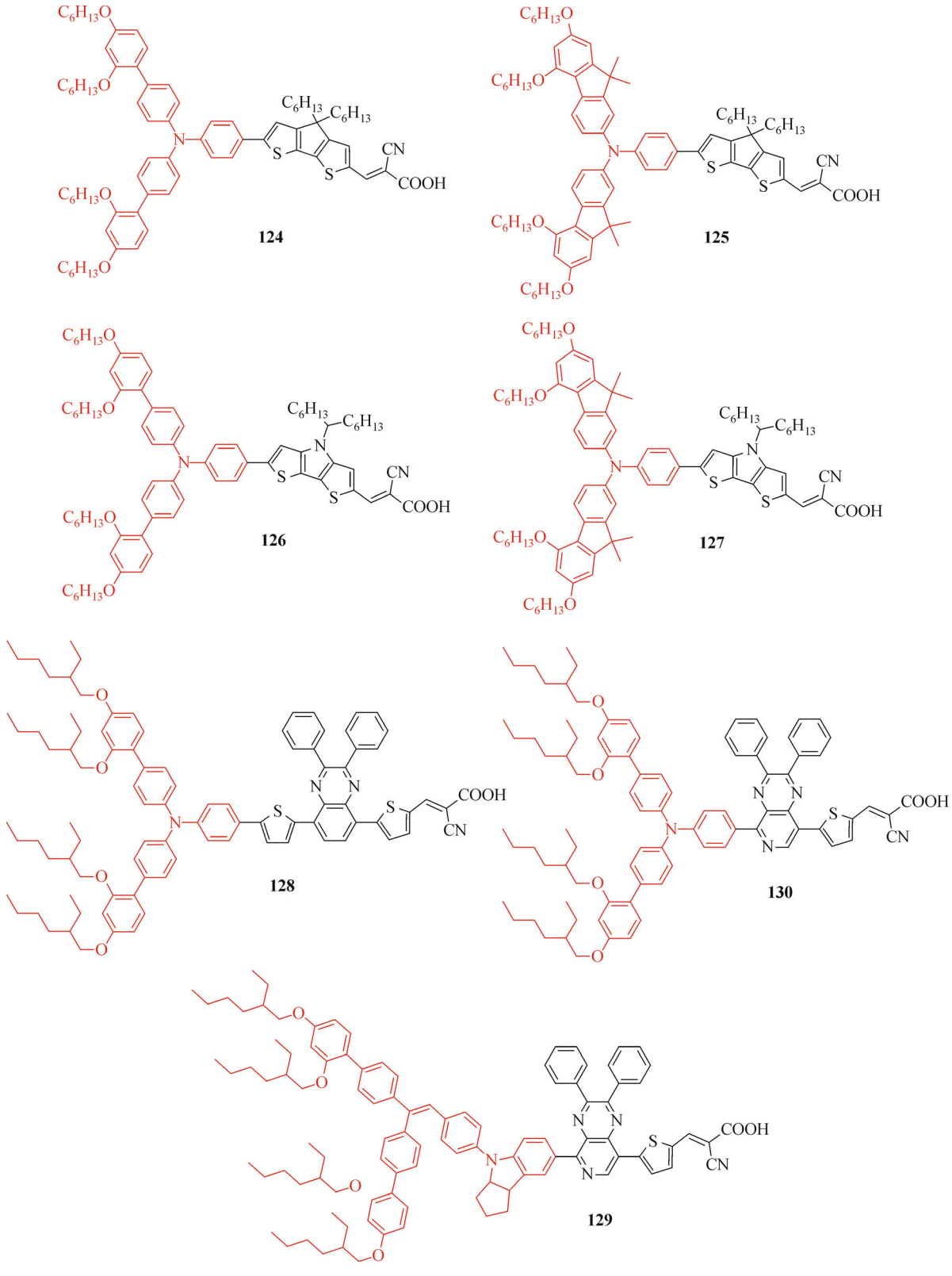

Scheme 15 Molecular structures of dyes **124**–**130**

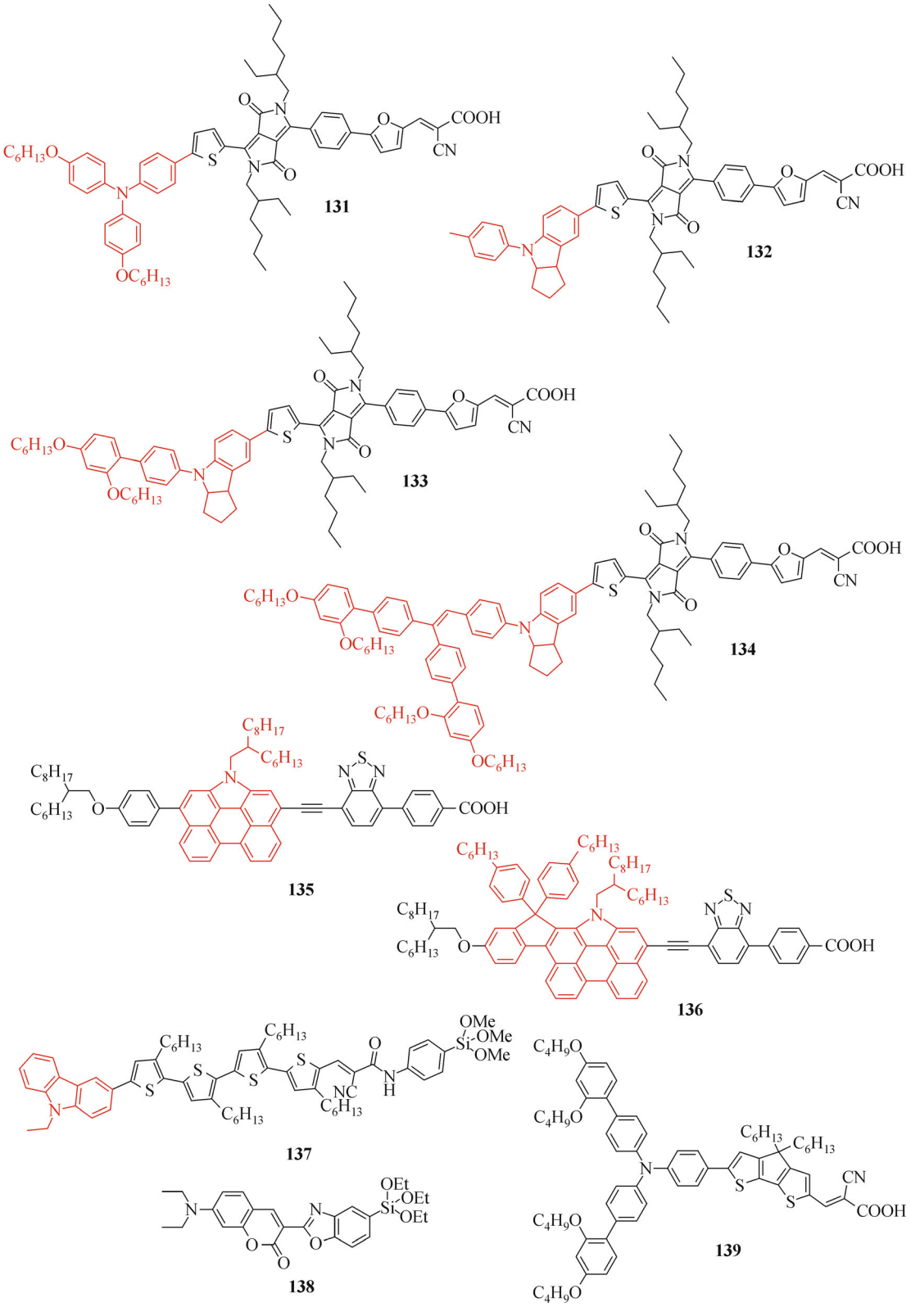

Scheme 16 Molecular structures of dyes **131**–**139**

a better light harvesting capability. Without any coadsorbent, DSSC based on **136** achieved a record PCE of 12.5% with high J_{sc} = 17.03 mA/cm^2, V_{oc} of 0.956 V and *FF* of 0.770 while PCE of 10.6% for DSSC based on **135** with J_{sc} = 15.81 mA/cm^2, V_{oc} of 0.897 V and *FF* of 0.744 under AM1.5G sunlight. The cobalt electrolyte employed was consist of 0.25 M $Co(phen)_3(TFSI)_2$, 0.05 M $Co(phen)_3(TFSI)_3$, 0.7 M TBP, and 0.05 M LiTFSI in acetonitrile [130].

Alkoxysilyl as the anchor group exhibited a strong bonding with TiO_2 and has been shown higher electron transfer efficiency, photovoltage and better stability than its counterpart of carboxy group. Carbozole dye **137** with alkoxysilyl anchor group has been demonstrated brilliant PCE of 12.49% in DSSC with J_{sc} = 15.57 mA/cm^2, V_{oc} = 1.036 V and *FF* = 0.775 using a cobalt(III/II)tris(5-chloro-1,10-phenanthroline)-based redox electrolyte containing 0.25 M $[Co(Cl\text{-}phen)_3]^{2+}(PF_6^-)_2$, 0.035 M $[Co(Cl\text{-}phen)_3]^{3+}(PF_6^-)_3$, 0.07 M $LiClO_4$, 0.02 M $NaClO_4$, 0.03 M tetrabutylammonium hexafluorophosphate (TBAPF), 0.01 M tetrabutylphosphonium hexafluorophosphate (TBPPF), 0.01M 1-hexyl-3-methylimidazolium hexafluorophosphate (HMImPF), 0.30 M TBP, 0.10 M 4-trimethylsilylpyridine (TMSP), 0.10 M 4-methylpyridine (MP) in acetonitrile. Recently, by co-sensitization with coumarin dye **138**, the maximum IPCE value of DSSC based on **137** reached 88%, offering a higher J_{sc} of 16.0 mA/cm^2, thus a high PCE of 12.81% has been made under the same condition [131]. Later they obtained a new record PCE of 14.3% with J_{sc} = 18.27 mA/cm^2, V_{oc} = 1.014 V and *FF* = 0.771 employing **139** as a co-sensitizer and $[Co(phen)_3]^{3+/2+}$ redox electrolyte in cooperated with Au + GNP counter electrodes [4].

4 Conclusion

In this review, we have summarized several useful strategies for donor design and modification of metal-free sensitizers for DSSCs and typical examples are presented (Tables 1 and 2). Basically, those strategies are aimed at improving the short-circuit current density and open-circuit voltage: adapting donors or adding additional donors for strong enough electron-donating ability, planar structure and adding electron-withdrawing groups for facilitating intramolecular charge transfer process, using blocking chains and twisted molecular structure for decreasing dye aggregation and charge recombination. Recently, new record photovoltaic conversion efficiencies of 10.2% for DSSCs with iodide electrolyte and 14.3% for DSSCs with cobalt electrolyte and co-sensitization have been made. New challenges for donor may focus on the

Table 1 Optical properties of mentioned dyes and their device performance with iodide/triiodide electrolyte

dye	λ_{max}[a] /nm	ε[a] /($M^{-1}\cdot cm^{-1}$)	λ_{max}[b] /nm	J_{sc} /($mA\cdot cm^{-2}$)	V_{oc}/V	*FF*	PCE/%	Ref.
1	464	32700		12.33	0.642	0.64	5.08	[30]
2	450	26900		11.46	0.643	0.66	4.93	[30]
3	497	37600		18.63	0.634	0.63	7.41	[30]
4	521	34000		13.7	0.606	0.69	5.7	[31]
5	491	36000		15.2	0.605	0.68	6.3	[31]
6	422	37700		16.81	0.74	0.57	7.08	[32]
7	427	29000		15.36	0.69	0.50	5.25	[32]
8	461	31300		14.28	0.71	0.60	6.12	[32]
9	461	27100		16.26	0.66	0.58	6.17	[32]
10	480	22200		11.88	0.58	0.54	3.74	[32]
11	468	22500		10.89	0.58	0.60	3.75	[32]
12	438	29420		13.0	0.66	0.71	6.00	[33]
13	455	20369		15.2	0.72	0.72	7.87	[33]
14	511	27900	459	8.92	0.630	0.79	4.44	[34]
15	558	42800	492	15.37	0.651	0.75	7.51	[34]
16	480	25000	505	13.8	0.632	0.69	6.02	[35]
17	422	29367	416	9.2	0.625	0.79	4.54	[36]
18	424	13834	424	7.3	0.603	0.74	3.26	[36]
19	442	13700	429	9.72	0.787	0.71	5.45	[37]
	415	20300	490	8.83	0.736	0.66	4.32	[43]

(*Continued*)

dye	λ_{max}[a)] /nm	ε[a)] /($M^{-1}\cdot cm^{-1}$)	λ_{max}[b)] /nm	J_{sc} /($mA\cdot cm^{-2}$)	V_{oc}/V	*FF*	PCE/%	Ref.
	474	28000	422	9.7	0.690	0.68	4.55	[60]
20	458	19800	440	11.33	0.792	0.71	6.38	[37]
21	479	21800	465	11.15	0.778	0.69	5.99	[37]
22	410	19400		8.88	0.764	0.560	3.80	[38]
23	425	27100		11.61	0.766	0.586	5.21	[38]
24	440	28400		11.71	0.709	0.592	4.92	[38]
25	460	24000	476	9.43	0.584	0.69	3.78	[39]
26	450	31000	475	10.84	0.592	0.69	4.41	[39]
27	449	23000	480	7.39	0.505	0.66	2.48	[39]
28	491	22300	471	11.63	0.639	0.68	5.08	[40]
29	523	27900	491	18.53	0.649	0.71	8.49	[40]
30	504	27200	490	15.29	0.627	0.72	6.84	[40]
31	523	58200		16.58	0.756	0.741	9.29	[41]
32	522	57100		16.28	0.779	0.748	9.49	[41]
33	492	33000	444	16.1	0.770	0.66	8.18	[42]
34	495	24000	423	14.8	0.723	0.66	7.06	[42]
35	465	21000	427	15.0	0.743	0.66	7.36	[42]
36	500	45000	448	15.8	0.775	0.66	8.08	[42]
37	447	27000	509	8.90	0.710	0.70	4.41	[43]
38	411	24300	483	8.45	0.753	0.70	4.44	[43]
39	436	30000		12.20	0.764	0.77	7.20	[44]
40	456	16000		15.33	0.74	0.66	7.43	[45]
41	463	25300		14.39	0.70	0.66	6.65	[46]
42	480	55000		13.84	0.790	0.75	8.2	[47]
43	480	73800		15.7	0.690	0.74	8.0	[48]
44	490	85000		17.61	0.710	0.72	9.1	[48]
45	550	31000	513	14.01	0.704	0.65	6.4	[49]
46	538	31000	487	13.37	0.714	0.66	6.3	[49]
47	542	38000	485	13.25	0.696	0.66	6.1	[49]
48	517	28000	468	14.90	0.738	0.69	7.5	[49]
49	472	26400	478	10.75	0.655	0.700	4.90	[50]
50	512	30100	484	16.50	0.734	0.684	8.28	[50]
51	498			7.66	0.946	0.658	4.76	[52]
52	482			10.1	0.893	0.681	6.15	[52]
53	490			16.5	0.833	0.737	10.1	[52]
54	513			11.8	0.832	0.703	6.91	[52]
55	444	20289		16.3	0.73	0.70	8.28	[33]
56	463	12614		16.8	0.75	0.70	8.71	[33]
57	482	70200	456	12.00	0.67	0.60	4.83	[54]
58	459	37200	446	12.50	0.71	0.59	5.24	[54]
59	445	70100	444	12.96	0.75	0.61	6.00	[54]
60	610	66111	632	11.76	0.464	0.674	3.7	[55]
61	615	88867	650	13.35	0.519	0.73	5.1	[56]
62	406	27500	422	7.75	0.689	0.73	3.90	[57]

(*Continued*)

dye	λ_{max}[a] /nm	ε[a] /($M^{-1}\cdot cm^{-1}$)	λ_{max}[b] /nm	J_{sc} /($mA\cdot cm^{-2}$)	V_{oc}/V	*FF*	PCE/%	Ref.
63	420	24900	425	7.89	0.731	0.74	4.27	[57]
64	430	41300	426	6.86	0.752	0.70	3.61	[57]
65	485	21600	441	10.359	0.715	0.722	5.35	[58]
66	468	34300	454	6.866	0.687	0.678	3.20	[58]
67	426	29000		12.21	0.65	0.59	4.68	[59]
68	413	21200		9.42	0.69	0.60	4.01	[59]
69	486	65000	443	9.8	0.750	0.67	4.92	[61]
70	498	52000	466	10.2	0.754	0.68	5.23	[60]
71	471	16000		11.82	0.759	0.65	5.84	[62]
72	474	20000		12.62	0.789	0.63	6.29	[62]
73	474	20000		11.41	0.804	0.63	5.76	[62]
74	412	16000		4.55	0.682	0.69	2.14	[63]
75	412	21000		5.27	0.711	0.72	2.69	[63]
76	462	13000		10.76	0.793	0.64	5.51	[63]
77	466	14000		12.18	0.826	0.65	6.55	[63]
78	518	22900		13.77	0.615	0.705	5.97	[73]
79	545	23600		16.91	0.672	0.717	8.15	[73]
80	536	37300	514	16.23	0.692	0.716	8.04	[74]
81	546	41000	529	12.32	0.699	0.727	6.27	[74]
82	551	43000	533	19.69	0.700	0.731	10.08	[74]
83	495	17200	428	13.39	0.68	0.74	6.74	[75]
84	496	19200	438	13.18	0.78	0.78	8.02	[75]
85	521	18700	508	13.60	0.685	0.67	6.24	[80]
86	523	21900	522	15.65	0.776	0.70	8.50	[80]
87	500	16700	479	7.10	0.570	0.76	3.11	[85]
88	497	16800	482	12.11	0.671	0.76	6.14	[85]
89	524	23300	516	13.56	0.691	0.76	7.12	[85]
90	514	41000		11.05	0.69	0.68	5.18	[95]
91	526	46000		13.40	0.76	0.73	7.43	[95]
92	593	33700	558	13.3	0.631	0.76	6.4	[89]
93	538	24100		17.1	0.642	0.675	7.4	[102]
94	549	55800		18.8	0.717	0.673	9.1	[102]
95	540	40300		12.7	0.730	0.712	6.6	[102]
96	556	33899		9.35	0.545	0.685	3.49	[103]
97	580	28840		12.32	0.595	0.708	5.19	[103]
98	584	23700		10.78	0.645	0.715	4.97	[103]
99	551	36399		12.10	0.610	0.728	5.37	[103]
100	492	36000	429	15.4	0.71	0.67	7.3	[104]
101	501	29900	437	15.5	0.70	0.62	6.7	[104]
102	427	50623	483	10.18	0.733	0.769	5.74	[105]
103	434	60782	470	7.89	0.767	0.765	4.63	[105]
104	423	39950		9.9	0.770	0.650	4.94	[106]
105	428	29680		9.3	0.739	0.689	4.73	[106]
106	426	33530		9.9	0.780	0.690	5.33	[106]

(*Continued*)

dye	λ_{max}[a] /nm	ε[a] /($M^{-1}\cdot cm^{-1}$)	λ_{max}[b] /nm	J_{sc} /($mA\cdot cm^{-2}$)	V_{oc}/V	*FF*	PCE/%	Ref.
107	443	40690		14.8	0.749	0.659	7.29	[106]
108	582	28000		15.4	0.730	0.75	8.4	[107]
109	598	33000		11.5	0.807	0.72	6.7	[107]
110	598	24000		13.3	0.716	0.70	6.7	[107]
111	531	12000		11.0	0.672	0.70	5.2	[107]
112	540	1600		3.7	0.553	0.78	1.7	[107]
113	484	27600	471	18.26	0.76	0.74	10.20	[108]
114	490	23000	484	16.76	0.76	0.76	9.67	[108]
115	498	19900	495	17.81	0.76	0.75	10.11	[108]
116	533	25900	553	18.82	0.71	0.72	9.69	[108]

Notes: a)—Absorption maximum wavelength and molar extinction coefficient in an organic solution. b)— Absorption maximum wavelength on TiO_2 film

Table 2 Optical properties of mentioned dyes and their device performance with cobalt electrolyte

dye	λ_{max}[a] /nm	ε[a] /($M^{-1}\cdot cm^{-1}$)	λ_{max}[b] /nm	J_{sc} /($mA\cdot cm^{-2}$)	V_{oc}/V	*FF*	PCE/%	Ref.
59	445	70100	444	10.7	0.92	0.68	6.7	[7]
117	526	17300	487	14.83	0.767	0.666	7.57	[119]
118	522	21400	502	15.58	0.797	0.712	8.84	[119]
119	534	27400	508	15.71	0.882	0.693	9.60	[119]
				16.25	0.890	0.737	10.65	
120	498	64000		12.0	0.830	0.72	7.2	[120]
121	500	81000		11.9	0.900	0.71	7.6	[121]
122	531	59200		14.32	0.907	0.68	8.83	[122]
123	543	69100		12.79	0.885	0.69	7.81	[122]
124	542	50500	441	14.6	0.855	0.70	8.8	[123]
				15.9	0.910	0.71	10.3	[124]
				14.1	0.876	0.78	9.8	[125]
125	548	47500	468	16.2	0.840	0.76	10.3	[125]
126	526	57700		13.4	0.901	0.74	8.86	[126]
127	541	52600		14.1	0.811	0.77	8.72	[127]
128	548	35528	539	16.75	0.830	0.706	9.81	[127]
129	557	26300	540	16.08	0.802	0.66	8.57	[127]
130	541	25500	532	15.35	0.790	0.64	7.74	[128]
131	587	55700		15.6	0.743	0.78	8.97	[129]
132	596	57100		15.2	0.716	0.76	8.23	[129]
133	600	62400		17.6	0.745	0.75	9.81	[129]
134	602	69000		17.9	0.761	0.74	10.1	[129]
135	512		507	15.81	0.897	0.744	10.6	[130]
136				17.03	0.956	0.770	12.5	[130]
137	498	43200		15.57	1.036	0.775	12.49	[131]
				15.99	1.034	0.774	12.81	[131]
				18.27	1.014	0.771	14.3	[4]

Notes: a)—Absorption maximum wavelength and molar extinction coefficient in an organic solution. b)— Absorption maximum wavelength on TiO_2 film

new design of panchromatic sensitizers and mechanics research.

Acknowledgements For financial support of this research, we thank the Science Fund for Creative Research Groups (21421004), the National Basic Research Program of China (973 Program) (No. 2013CB733700), and the National Natural Science Foundation of China (Grant Nos. 21172073, 21372082, 21572062 and 91233207). J.-L. Hua appreciates Prof. H. Tian very much for his helpful discussion and valuable comments.

References

1. Grätzel M. Conversion of sunlight to electric power by nanocrystalline dye-sensitized solar cells. Journal of Photochemistry and Photobiology A Chemistry, 2004, 164(1–3): 3–14
2. Hagfeldt A, Boschloo G, Sun L, Kloo L, Pettersson H. Dye-sensitized solar cells. Chemical Reviews, 2010, 110(11): 6595–6663
3. Ye M D, Wen X R, Wang M Y, Iocozzia J, Zhang N, Lin C J, Lin Z Q. Recent advances in dye-sensitized solar cells: from photoanodes, sensitizers and electrolytes to counter electrodes. Materials Today, 2015, 18(3): 155–162
4. Kakiage K, Aoyama Y, Yano T, Oya K, Fujisawa J, Hanaya M. Highly-efficient dye-sensitized solar cells with collaborative sensitization by silyl-anchor and carboxy-anchor dyes. Chemical Communications, 2015, 51(88): 15894–15897
5. O'Regan B, Grätzel M. A low-cost, high-efficiency solar cell based on dye-sensitized colloidal TiO_2 films. Nature, 1991, 353(6346): 737–740
6. Boschloo G, Hagfeldt A. Characteristics of the iodide/triiodide redox mediator in dye-sensitized solar cells. Accounts of Chemical Research, 2009, 42(11): 1819–1826
7. Feldt S M, Gibson E A, Gabrielsson E, Sun L, Boschloo G, Hagfeldt A. Design of organic dyes and cobalt polypyridine redox mediators for high-efficiency dye-sensitized solar cells. Journal of the American Chemical Society, 2010, 132(46): 16714–16724
8. Feldt S M, Wang G, Boschloo G, Hagfeldt A. Effects of driving forces for recombination and regeneration on the photovoltaic performance of dye-sensitized solar cells using cobalt polypyridine redox couples. Journal of Physical Chemistry C, 2011, 115(43): 21500–21507
9. Feldt S M, Lohse P W, Kessler F, Nazeeruddin M K, Grätzel M, Boschloo G, Hagfeldt A. Regeneration and recombination kinetics in cobalt polypyridine based dye-sensitized solar cells, explained using Marcus theory. Physical Chemistry Chemical Physics, 2013, 15(19): 7087–7097
10. Jennings J R, Ghicov A, Peter L M, Schmuki P, Walker A B. Dye-sensitized solar cells based on oriented TiO_2 nanotube arrays: transport, trapping, and transfer of electrons. Journal of the American Chemical Society, 2008, 130(40): 13364–13372
11. Jennings J R, Liu Y R, Wang Q. Efficiency limitations in dye-sensitized solar cells caused by inefficient sensitizer regeneration. Journal of Physical Chemistry C, 2011, 115(30): 15109–15120
12. Nazeeruddin M K, Kay A, Rodicio I, Humpbry-Baker R, Miiller E, Liska P, Vlachopoulos N, Grätzel M. Conversion of light to electricity by cis-X_2Bis(2,2′-bipyridyl-4,4′-dicarboxylate)ruthenium(II) charge-transfer sensitizers (X = Cl^-, Br^-, I^-, CN^-, and SCN^-) on nanocrystalline TiO_2 electrodes. Journal of the American Chemical Society, 1993, 115(14): 6382–6390
13. Grätzel M. Dye-sensitized solar cells. Journal of Photochemistry and Photobiology C, Photochemistry Reviews, 2003, 4(2): 145–153
14. Wang M K, Grätzel C, Zakeeruddin S M, Grätzel M. Recent developments in redox electrolytes for dye-sensitized solar cells. Energy & Environmental Science, 2012, 5(11): 9394–9405
15. Katoh R, Kasuya M, Kodate S, Furube A, Fuke N, Koide N. Effects of 4-tert-butylpyridine and Li ions on photoinduced electron injection efficiency in black-dye-sensitized nanocrystalline TiO_2 films. Journal of Physical Chemistry C, 2009, 113(48): 20738–20744
16. Lu H P, Tsai C Y, Yen W N, Hsieh C P, Lee C W, Yeh C Y, Diau E W G. Control of dye aggregation and electron injection for highly efficient porphyrin sensitizers adsorbed on semiconductor films with varying ratios of coadsorbate. Journal of Physical Chemistry C, 2009, 113(49): 20990–20997
17. Gregg B A, Pichot F, Ferrere S, Fields C L. Interfacial recombination processes in dye-sensitized solar cells and methods to passivate the interfaces. Journal of Physical Chemistry B, 2001, 105(7): 1422–1429
18. Park J, Yi J, Tachikawa T, Majima T, Choi W. Guanidinium-enhanced production of hydrogen on nafion-coated dye/TiO_2 under visible light. Journal of Physical Chemistry Letters, 2010, 1(9): 1351–1355
19. Ahmad S, Guillén E, Kavan L, Grätzel M, Nazeeruddin M K. Metal free sensitizer and catalyst for dye sensitized solar cells. Energy & Environmental Science, 2013, 6(12): 3439–3466
20. Hamann T W, Jensen R A, Martinson A B F, Van Ryswyk H, Hupp J T. Advancing beyond current generation dye-sensitized solar cells. Energy & Environmental Science, 2008, 1(1): 66–78
21. Chiba Y, Islam A, Watanabe Y, Komiya R, Koide N, Han L. Dye-sensitized solar cells with conversion efficiency of 11.1%. Japanese Journal of Applied Physics, 2006, 45(25): 638–640
22. Nazeeruddin M K, Péchy P, Renouard T, Zakeeruddin S M, Humphry-Baker R, Comte P, Liska P, Cevey L, Costa E, Shklover V, Spiccia L, Deacon G B, Bignozzi C A, Grätzel M. Engineering of efficient panchromatic sensitizers for nanocrystalline $TiO_{(2)}$-based solar cells. Journal of the American Chemical Society, 2001, 123(8): 1613–1624
23. Yella A, Lee H W, Tsao H N, Yi C, Chandiran A K, Nazeeruddin M K, Diau E W G, Yeh C Y, Zakeeruddin S M, Grätzel M. Porphyrin-sensitized solar cells with cobalt (II/III)-based redox electrolyte exceed 12 percent efficiency. Science, 2011, 334(6056): 629–634
24. Mathew S, Yella A, Gao P, Humphry-Baker R, Curchod B F E, Ashari-Astani N, Tavernelli I, Rothlisberger U, Nazeeruddin M K, Grätzel M. Dye-sensitized solar cells with 13% efficiency achieved through the molecular engineering of porphyrin sensitizers. Nature Chemistry, 2014, 6(3): 242–247
25. Yao Z, Zhang M, Wu H, Yang L, Li R, Wang P. Donor/acceptor indenoperylene dye for highly efficient organic dye-sensitized solar cells. Journal of the American Chemical Society, 2015, 137 (11): 3799–3802

26. Kakiage K, Aoyama Y, Yano T, Oya K, Kyomen T, Hanaya M. Fabrication of a high-performance dye-sensitized solar cell with 12.8% conversion efficiency using organic silyl-anchor dyes. Chemical Communications, 2015, 51(29): 6315–6317
27. Mishra A, Fischer M K R, Bäuerle P. Metal-free organic dyes for dye-sensitized solar cells: from structure: property relationships to design rules. Angewandte Chemie International Edition, 2009, 48 (14): 2474–2499
28. Liang M, Chen J. Arylamine organic dyes for dye-sensitized solar cells. Chemical Society Reviews, 2013, 42(8): 3453–3488
29. Clifford J N, Martínez-Ferrero E, Viterisi A, Palomares E. Sensitizer molecular structure-device efficiency relationship in dye sensitized solar cells. Chemical Society Reviews, 2011, 40(3): 1635–1646
30. Liu B, Zhu W, Zhang Q, Wu W, Xu M, Ning Z, Xie Y, Tian H. Conveniently synthesized isophorone dyes for high efficiency dye-sensitized solar cells: tuning photovoltaic performance by structural modification of donor group in donor-π-acceptor system. Chemical Communications, 2009, 13(13): 1766–1768
31. Cheng X B, Sun S Y, Liang M, Shi Y B, Sun Z, Xue S. Organic dyes incorporating the cyclopentadithiophene moiety for efficient dye-sensitized solar cells. Dyes and Pigments, 2012, 92(3): 1292–1299
32. Chang Y J, Chow T J. Dye-sensitized solar cell utilizing organic dyads containing triarylene conjugates. Tetrahedron, 2009, 65(24): 4726–4734
33. Do K, Kim D, Cho N, Paek S, Song K, Ko J. New type of organic sensitizers with a planar amine unit for efficient dye-sensitized solar cells. Organic Letters, 2012, 14(1): 222–225
34. Cai L P, Tsao H N, Zhang W, Wang L, Xue Z S, Grätzel M, Liu B. Organic sensitizers with bridged triphenylamine donor units for efficient dye-sensitized solar cells. Advanced Energy Materials, 2013, 3(2): 200–205
35. Ning Z, Zhang Q, Wu W, Pei H, Liu B, Tian H. Starburst triarylamine based dyes for efficient dye-sensitized solar cells. Journal of Organic Chemistry, 2008, 73(10): 3791–3797
36. Wan Z Q, Jia C Y, Duan Y D, Zhou L L, Zhang J Q, Lin Y, Shi Y. Influence of the antennas in starburst triphenylamine-based organic dyesensitized solar cells: phenothiazine versus carbazole. RSC Advances, 2012, 2(10): 4507–4514
37. Chai Q P, Li W Q, Zhu S Q, Zhang Q, Zhu W H. Influence of donor configurations on photophysical electrochemical, and photovoltaic performances in D-π-A organic sensitizers. ACS Sustainable Chemistry & Engineering, 2014, 2(2): 239–247
38. Zhang M D, Pan H, Ju X H, Ji Y J, Qin L, Zheng H G, Zhou X F. Improvement of dye-sensitized solar cells' performance through introducing suitable heterocyclic groups to triarylamine dyes. Physical Chemistry Chemical Physics, 2012, 14(8): 2809–2815
39. Wu W J, Yang J B, Hua J L, Tang J, Zhang L, Long Y T, Tian H. Efficient and stable dye-sensitized solar cells based on phenothiazine sensitizers with thiophene units. Journal of Materials Chemistry, 2010, 20(9): 1772–1779
40. Liu B, Liu Q B, You D, Li X Y, Naruta Y, Zhu W H. Molecular engineering of indoline based organic sensitizers for highly efficient dye-sensitized solar cells. Journal of Materials Chemistry, 2012, 22(26): 13348–13356
41. Liu B, Wang B, Wang R, Gao L, Huo S H, Liu Q B, Li X Y, Zhu W H. Influence of conjugated π-linker in D-D-π-A indoline dyes: towards long-term stable and efficient dye-sensitized solar cells with high photovoltage. Journal of Materials Chemistry A, Materials for Energy and Sustainability, 2014, 2(3): 804–812
42. Li G, Liang M, Wang H, Sun Z, Wang L N, Wang Z H, Xue S. Significant enhancement of open-circuit voltage in indoline-based dye-sensitized solar cells via retarding charge recombination. Chemistry of Materials, 2013, 25(9): 1713–1722
43. Tang J, Hua J L, Wu W J, Li J, Jin Z G, Long Y T, Tian H. New starburst sensitizer with carbazole antennas for efficient and stable dye-sensitized solar cells. Energy & Environmental Science, 2010, 3(11): 1736–1745
44. Kim S, Lee J K, Kang S O, Ko J, Yum J H, Fantacci S, De Angelis F, Di Censo D, Nazeeruddin M K, Grätzel M. Molecular engineering of organic sensitizers for solar cell applications. Journal of the American Chemical Society, 2006, 128(51): 16701–16707
45. Choi H, Lee J K, Song K, Kang S O, Ko J. Novel organic dyes containing bis-dimethylfluorenyl amino benzo[*b*]thiophene for highly efficient dye-sensitized solar cell. Tetrahedron, 2007, 63 (15): 3115–3121
46. Jung I, Lee J K, Song K H, Song K, Kang S O, Ko J. Synthesis and photovoltaic properties of efficient organic dyes containing the benzo[*b*]furan moiety for solar cells. Journal of Organic Chemistry, 2007, 72(10): 3652–3658
47. Lim K, Kim C, Song J, Yu T, Lim W, Song K, Wang P, Zu N N, Ko J. Enhancing the performance of organic dye-sensitized solar cells via a slight structure modification. Journal of Physical Chemistry C, 2011, 115(45): 22640–22646
48. Choi H, Raabe I, Kim D, Teocoli F, Kim C, Song K, Yum J H, Ko J, Nazeeruddin M K, Grätzel M. High molar extinction coefficient organic sensitizers for efficient dye-sensitized solar cells. Chemistry—A European Journal, 2010, 16(4): 1193–1201
49. Liu J, Yang X C, Zhao J X, Sun L C. Tuning band structures of dyes for dye-sensitized solar cells: effect of different π-bridges on the performance of cells. RSC Advances, 2013, 3(36): 15734–15743
50. Yang L, Zheng Z, Li Y, Wu W, Tian H, Wang Z. *N*-Annulated perylene-based metal-free organic sensitizers for dye-sensitized solar cells. Chemical Communications, 2015, 51(23): 4842–4845
51. Facchetti A. π-Conjugated polymers for organic electronics and photovoltaic cell applications. Chemistry of Materials, 2011, 23(3): 733–758
52. Zhou N, Prabakaran K, Lee B, Chang S H, Harutyunyan B, Guo P, Butler M R, Timalsina A, Bedzyk M J, Ratner M A, Vegiraju S, Yau S, Wu C G, Chang R P H, Facchetti A, Chen M C, Marks T J. Metal-free tetrathienoacene sensitizers for high-performance dye-sensitized solar cells. Journal of the American Chemical Society, 2015, 137(13): 4414–4423
53. Buhbut S, Clifford J N, Kosa M, Anderson A Y, Shalom M, Major D T, Palomares E, Zaban A. Controlling dye aggregation, injection energetics and catalytic recombination in organic sensitizer based dye cells using a single electrolyte additive. Energy & Environmental Science, 2013, 6(10): 3046–3053
54. Hagberg D P, Jiang X, Gabrielsson E, Linder M, Marinado T,

Brinck T, Hagfeldt A, Sun L C. Symmetric and unsymmetric donor functionalization: comparing structural and spectral benefits of chromophores for dye-sensitized solar cells. Journal of Materials Chemistry, 2009, 19(39): 7232–7238

55. Hao Y, Yang X, Cong J, Tian H, Hagfeldt A, Sun L. Efficient near infrared D-π-A sensitizers with lateral anchoring group for dye-sensitized solar cells. Chemical Communications, 2009, 27(27): 4031–4033
56. Hao Y, Yang X, Zhou M, Cong J, Wang X, Hagfeldt A, Sun L. Molecular design to improve the performance of donor-π acceptor near-IR organic dye-sensitized solar cells. ChemSusChem, 2011, 4 (11): 1601–1605
57. Ning Z J, Zhang Q, Pei H C, Luan J F, Lu C G, Cui Y P, Tian H. Photovoltage improvement for dye-sensitized solar cells via cone-shaped structural design. Journal of Physical Chemistry C, 2009, 113(23): 10307–10313
58. Numata Y, Islam A, Chen H, Han L Y. Aggregation-free branch-type organic dye with a twisted molecular architecture for dye-sensitized solar cells. Energy & Environmental Science, 2012, 5 (9): 8548–8552
59. Tsai M S, Hsu Y C, Lin J T, Chen H C, Hsu C P. Organic dyes containing 1H-phenanthro[9,10-d]imidazole conjugation for solar cells. Journal of Physical Chemistry C, 2007, 111(50): 18785–18793
60. Lu M, Liang M, Han H Y, Sun Z, Xue S. Organic dyes incorporating bis-hexapropyltruxeneamino moiety for efficient dye-sensitized solar cells. Journal of Physical Chemistry C, 2011, 115(1): 274–281
61. Liang M, Lu M, Wang Q L, Chen W Y, Han H Y, Sun Z, Xue S. Efficient dye-sensitized solar cells with triarylamine organic dyes featuring functionalized-truxene unit. Journal of Power Sources, 2011, 196(3): 1657–1664
62. Chen C J, Liao J Y, Chi Z G, Xu B J, Zhang X Q, Kuang D B, Zhang Y, Liu S W, Xu J R. Effect of polyphenyl-substituted ethylene end-capped groups in metal-free organic dyes on performance of dye-sensitized solar cells. RSC Advances, 2012, 2(20): 7788–7797
63. Chen C J, Liao J Y, Chi Z G, Xu B J, Zhang X Q, Kuang D B, Zhang Y, Liu S W, Xu J R. Metal-free organic dyes derived from triphenylethylene for dye-sensitized solar cells: tuning of the performance by phenothiazine and carbazole. Journal of Materials Chemistry, 2012, 22(18): 8994–9005
64. Wu Y, Zhu W. Organic sensitizers from D-π-A to D-A-π-A: effect of the internal electron-withdrawing units on molecular absorption, energy levels and photovoltaic performances. Chemical Society Reviews, 2013, 42(5): 2039–2058
65. Wu Y, Zhu W H, Zakeeruddin S M, Grätzel M. Insight into D-A-π-A structured sensitizers: a promising route to highly efficient and stable dye-sensitized solar cells. ACS Applied Materials & Interfaces, 2015, 7(18): 9307–9318
66. Velusamy M, Justin Thomas K R, Lin J T, Hsu Y C, Ho K C. Organic dyes incorporating low-band-gap chromophores for dye-sensitized solar cells. Organic Letters, 2005, 7(10): 1899–1902
67. Zhu W H, Wu Y Z, Wang S T, Li W Q, Li X, Chen J, Wang Z S, Tian H. Organic D-A-π-A solar cell sensitizers with improved stability and spectral response. Advanced Functional Materials, 2011, 21(4): 756–763
68. Wu Y Z, Zhang X, Li W Q, Wang Z S, Tian H, Zhu W H. Hexylthiophene-featured D-A-π-A structural indoline chromophores for coadsorbent-free and panchromatic dye-sensitized solar cells. Advanced Energy Materials, 2012, 2(1): 149–156
69. Wu Y Z, Marszalek M, Zakeeruddin S M, Zhang Q, Tian H, Grätzel M, Zhu W H. High-conversion-efficiency organic dye-sensitized solar cells: molecular engineering on D-A-π-A featured organic indoline dyes. Energy & Environmental Science, 2012, 5 (8): 8261–8272
70. Zhu H B, Li W Q, Wu Y Z, Liu B, Zhu S Q, Li X, Ågren H, Zhu W H. Insight into benzothiadiazole acceptor in D-A-π-A configuration on photovoltaic performances of dye-sensitized solar cells. ACS Sustainable Chemistry & Engineering, 2014, 2(4): 1026–1034
71. Chen L, Li X, Ying W J, Zhang X Y, Guo F L, Li J, Hua J L. 5,6-Bis(octyloxy)benzo[*c*][1,2,5]thiadiazole-bridged dyes for dye-sensitized solar cells with high open-circuit voltage performance. European Journal of Organic Chemistry, 2013, 2013(9): 1770–1780
72. Zhang X Y, Chen L, Li X, Mao J, Wu W, Ågren H, Hua J. Photovoltaic properties of bis(octyloxy)benzo-[*c*][1,2,5]thiadiazole sensitizers based on an *N, N*-diphenylthiophen-2-amine donor. Journal of Materials Chemistry C, Materials for Optical and Electronic Devices, 2014, 2(20): 4063–4072
73. Zhu H B, Li W Q, Wu Y Z, Liu B, Zhu S Q, Li X, Ågren H, Zhu W H. Insight into benzothiadiazole acceptor in D-A-π-A configuration on photovoltaic performances of dye-sensitized solar cells. ACS Sustainable Chemistry & Engineering, 2014, 2(4): 1026–1034
74. Chai Q P, Li W Q, Liu J C, Geng Z Y, Tian H.Zhu W H.Rational molecular engineering of cyclopentadithiophene-bridged D-A-π-A sensitizers combining high photovoltaic efficiency with rapid dye adsorption. Scientific Reports, 2015, 5: 11330
75. Cui Y, Wu Y Z, Lu X F, Zhang X, Zhou G, Miapeh F B, Zhu W H, Wang Z S. Incorporating benzotriazole moiety to construct D-A-π-A organic sensitizers for solar cells: significant enhancement of open-circuit photovoltage with long alkyl group. Chemistry of Materials, 2011, 23(19): 4394–4401
76. Mao J, Guo F, Ying W, Wu W, Li J, Hua J. Benzotriazole-bridged sensitizers containing a furan moiety for dye-sensitized solar cells with high open-circuit voltage performance. Chemistry, an Asian Journal, 2012, 7(5): 982–991
77. Yen Y S, Lee C T, Hsu C Y, Chou H H, Chen Y C, Lin J T. Benzotriazole-containing D-π-A conjugated organic dyes for dye-sensitized solar cells. Chemistry, an Asian Journal, 2013, 8(4): 809–816
78. Chai Q, Li W, Wu Y, Pei K, Liu J, Geng Z, Tian H, Zhu W. Effect of a long alkyl group on cyclopentadithiophene as a conjugated bridge for D-A-π-A organic sensitizers: IPCE, electron diffusion length, and charge recombination. ACS Applied Materials & Interfaces, 2014, 6(16): 14621–14630
79. Li H, Wu Y Z, Geng Z Y, Liu J C, Xu D D, Zhu W H. Co-sensitization of benzoxadiazole based D-A-π-A featured sensitizers: compensating light-harvesting and retarding charge recombination. Journal of Materials Chemistry. A, Materials for Energy

and Sustainability, 2014, 2(35): 14649–14657
80. Pei K, Wu Y, Wu W, Zhang Q, Chen B, Tian H, Zhu W. Constructing organic D-A-π-A-featured sensitizers with a quinoxaline unit for high-efficiency solar cells: the effect of an auxiliary acceptor on the absorption and the energy level alignment. Chemistry—A European Journal, 2012, 18(26): 8190–8200
81. Pei K, Wu Y, Islam A, Zhang Q, Han L, Tian H, Zhu W. Constructing high-efficiency D-A-π-A-featured solar cell sensitizers: a promising building block of 2,3-diphenylquinoxaline for antiaggregation and photostability. ACS Applied Materials & Interfaces, 2013, 5(11): 4986–4995
82. Pei K, Wu Y Z, Islam A, Zhu S Q, Han L Y, Geng Z Y, Zhu W H. Dye-sensitized solar cells based on quinoxaline dyes: effect of π-linker on absorption, energy levels, and photovoltaic performances. Journal of Physical Chemistry C, 2014, 118(30): 16552–16561
83. Pei K, Wu Y, Li H, Geng Z, Tian H, Zhu W H. Cosensitization of D-A-π-A quinoxaline organic dye: efficiently filling the absorption valley with high photovoltaic efficiency. ACS Applied Materials & Interfaces, 2015, 7(9): 5296–5304
84. Chang D W, Lee H J, Kim J H, Park S Y, Park S M, Dai L, Baek J B. Novel quinoxaline-based organic sensitizers for dye-sensitized solar cells. Organic Letters, 2011, 13(15): 3880–3883
85. Ying W J, Yang J B, Wielopolski M, Moehl T, Moser J E, Comte P, Hua J L, Zakeeruddin S M, Tian H, Grätzel M. New pyrido[3,4-*b*]pyrazine-based sensitizers for efficient and stable dye-sensitized solar cells. Chemical Science (Cambridge), 2014, 5(1): 206–214
86. Li X, Cui S, Wang D, Zhou Y, Zhou H, Hu Y, Liu J G, Long Y, Wu W, Hua J, Tian H. New organic donor-acceptor-π-acceptor sensitizers for efficient dye-sensitized solar cells and photocatalytic hydrogen evolution under visible-light irradiation. ChemSusChem, 2014, 7(10): 2879–2888
87. Zhang X Y, Ying W J, Wu W J, Li J, Hua J L. Synthesis and photovoltaic performance of (octyloxyphenyl)pyrido-[3,4-*b*]pyrazine-based sensitizers for dye-sensitized solar cells. Acta Chimica Sinica, 2015, 73(3): 272–280
88. Ying W J, Zhang X Y, Li X, Wu W J, Guo F L, Li J, Ågren H, Hua J L. Synthesis and photovoltaic properties of new [1,2,5]thiadiazolo[3,4-*c*]pyridine-based organic Broadly absorbing sensitizers for dye-sensitized solar cells. Tetrahedron, 2014, 70(25): 3901–3908
89. Mao J, Yang J, Teuscher J, Moehl T, Yi C, Humphry-Baker R, Comte P, Grätzel C, Hua J, Zakeeruddin S M, Tian H, Grätzel M. Thiadiazolo[3,4-*c*]pyridine acceptor based blue sensitizers for high efficiency dye-sensitized solar cells. Journal of Physical Chemistry C, 2014, 118(30): 17090–17099
90. Hua Y, He J, Zhang C S, Qin C J, Han L Y, Zhao J Z, Chen T, Wong W Y, Wong W K, Zhu X J. Effects of various π-conjugated spacers in thiadiazole[3,4-*c*]pyridine-cored panchromatic organic dyes for dye-sensitized solar cells. Journal of Materials Chemistry A, Materials for Energy and Sustainability, 2015, 3(6): 3103–3112
91. Feng Q, Lu X, Zhou G, Wang Z S. Synthesis and photovoltaic properties of organic sensitizers incorporating a thieno[3,4-*c*]pyrrole-4,6-dione moiety. Physical Chemistry Chemical Physics, 2012, 14(22): 7993–7999
92. Feng Q, Zhang W, Zhou G, Wang Z S. Enhanced performance of quasi-solid-state dye-sensitized solar cells by branching the linear substituent in sensitizers based on thieno[3,4-*c*]pyrrole-4,6-dione. Chemistry, an Asian Journal, 2013, 8(1): 168–177
93. Qu S Y, Wu W J, Hua J L, Kong C, Long Y T, Tian H. New diketopyrrolopyrrole (DPP) dyes for efficient dye-sensitized solar cells. Journal of Physical Chemistry C, 2010, 114(2): 1343–1349
94. Qu S, Qin C, Islam A, Hua J, Chen H, Tian H, Han L. Tuning the electrical and optical properties of diketopyrrolopyrrole complexes for panchromatic dye-sensitized solar cells. Chemistry, an Asian Journal, 2012, 7(12): 2895–2903
95. Qu S, Qin C, Islam A, Wu Y, Zhu W, Hua J, Tian H, Han L. A novel D-A-π-A organic sensitizer containing a diketopyrrolopyrrole unit with a branched alkyl chain for highly efficient and stable dye-sensitized solar cells. Chemical Communications, 2012, 48 (55): 6972–6974
96. Qu S Y, Hua J L, Tian H. New D-π-A dyes for efficient dye-sensitized solar cells. Science China Chemistry, 2012, 55(5): 677–697
97. Qu S Y, Wang B, Guo F L, Li J, Wu W J, Kong C, Long Y T, Hua J L. New diketo-pyrrolo-pyrrole (DPP) sensitizer containing a furan moiety for efficient and stable dye-sensitized solar cells. Dyes and Pigments, 2012, 92(3): 1384–1393
98. Holcombe T W, Yum J H, Kim Y, Rakstys K, Grätzel M. Diketopyrrolopyrrole-based sensitizers for dye-sensitized solar cell applications: anchor engineering. Journal of Materials Chemistry A, Materials for Energy and Sustainability, 2013, 1(44): 13978–13983
99. Ying W, Guo F, Li J, Zhang Q, Wu W, Tian H, Hua J. Series of new D-A-π-A organic broadly absorbing sensitizers containing isoindigo unit for highly efficient dye-sensitized solar cells. ACS Applied Materials & Interfaces, 2012, 4(8): 4215–4224
100. Li S G, Jiang K J, Huang J H, Yang L M, Song Y L. Molecular engineering of panchromatic isoindigo sensitizers for dye-sensitized solar cell applications. Chemical Communications, 2014, 50(33): 4309–4311
101. Wang D, Ying W J, Zhang X Y, Hu Y, Wu W J, Hua J L. Near-infrared absorbing isoindigo sensitizers: synthesis and performance for dye-sensitized solar cells. Dyes and Pigments, 2015, 112: 327–334
102. Kang X W, Zhang J X, O'Neil D, Rojas A J, Chen W, Szymanski P, Marder S R, El-Sayed M A. Effect of molecular structure perturbations on the performance of the D-A-π-A dye sensitized solar cells. Chemistry of Materials, 2014, 26(15): 4486–4493
103. Franco S, Garín J, de Baroja N M, Pérez-Tejada R, Orduna J, Yu Y, Lira-Cantú M. New D-π-A-conjugated organic sensitizers based on 4*H*-pyran-4-ylidene donors for highly efficient dye-sensitized solar cells. Organic Letters, 2012, 14(3): 752–755
104. Zhang X H, Wang Z S, Cui Y, Koumura N, Furube A, Hara K. Organic sensitizers based on hexylthiophene-functionalized indolo[3,2-*b*]carbazole for efficient dye-sensitized solar cells. Journal of Physical Chemistry C, 2009, 113(30): 13409–13415
105. Paramasivam M, Chitumalla R K, Singh S P, Islam A, Han L Y, Rao V J, Bhanuprakash K. Tuning the photovoltaic performance of benzocarbazole-based sensitizers for dye-sensitized solar cells: a joint experimental and theoretical study of the influence of π-spacers. Journal of Physical Chemistry C, 2015, 119(30): 17053–

17064

106. Wu Z, An Z, Chen X, Chen P. Cyclic thiourea/urea functionalized triphenylamine-based dyes for high-performance dye-sensitized solar cells. Organic Letters, 2013, 15(7): 1456–1459
107. Delcamp J H, Yella A, Holcombe T W, Nazeeruddin M K, Grätzel M. The molecular engineering of organic sensitizers for solar-cell applications. Angewandte Chemie International Edition, 2013, 52 (1): 376–380
108. Joly D, Pellejà L, Narbey S, Oswald F, Meyer T, Kervella Y, Maldivi P, Clifford J N, Palomares E, Demadrille R. Metal-free organic sensitizers with narrow absorption in the visible for solar cells exceeding 10% efficiency. Energy & Environmental Science, 2015, 8(7): 2010–2018
109. Hardin B E, Snaith H J, McGehee M D. The renaissance of dye-sensitized solar cells. Nature Photonics, 2012, 6(3): 162–169
110. Cheng M, Yang X, Chen C, Zhao J, Zhang F, Sun L. Dye-sensitized solar cells based on hydroquinone/benzoquinone as bio-inspired redox couple with different counter electrodes. Physical Chemistry Chemical Physics, 2013, 15(36): 15146–15152
111. Tian H N, Gabrielsson E, Lohse P W, Vlachopoulos N, Kloo L, Hagfeldt A, Sun L C. Development of an organic redox couple and organic dyes for aqueous dye-sensitized solar cells. Energy & Environmental Science, 2012, 5(12): 9752–9755
112. Bai Y, Yu Q, Cai N, Wang Y, Zhang M, Wang P. High-efficiency organic dye-sensitized mesoscopic solar cells with a copper redox shuttle. Chemical Communications, 2011, 47(15): 4376–4378
113. Wang M, Chamberland N, Breau L, Moser J E, Humphry-Baker R, Marsan B, Zakeeruddin S M, Grätzel M. An organic redox electrolyte to rival triiodide/iodide in dye-sensitized solar cells. Nature Chemistry, 2010, 2(5): 385–389
114. Sun Z, Liang M, Chen J. Kinetics of iodine-free redox shuttles in dye-Sensitized solar cells: interfacial recombination and dye regeneration. Accounts of Chemical Research, 2015, 48(6): 1541–1550
115. Nusbaumer H, Moser J E, Zakeeruddin S M, Nazeeruddin M K, Grätzel M. $Co^{II}(dbbip)_2^{2+}$ Complex rivals tri-iodide/iodide redox mediator in dye-sensitized photovoltaic cells. Journal of Physical Chemistry B, 2001, 105(43): 10461–10464
116. Yum J H, Baranoff E, Kessler F, Moehl T, Ahmad S, Bessho T, Marchioro A, Ghadiri E, Moser J E, Yi C Y, Nazeeruddin M K, Grätzel M. A cobalt complex redox shuttle for dye-sensitized solar cells with high open-circuit potentials. Nature Communications, 2012, 3: 631
117. Kashif M K, Axelson J C, Duffy N W, Forsyth C M, Chang C J, Long J R, Spiccia L, Bach U. A new direction in dye-sensitized solar cells redox mediator development: in situ fine-tuning of the cobalt(II)/(III) redox potential through Lewis base interactions. Journal of the American Chemical Society, 2012, 134(40): 16646–16653
118. Tsao H N, Comte P, Yi C, Grätzel M. Avoiding diffusion limitations in cobalt(III/II)-tris(2,2′-bipyridine)-based dye-sensitized solar cells by tuning the mesoporous TiO_2 film properties. ChemPhysChem, 2012, 13(12): 2976–2981
119. Yang J, Ganesan P, Teuscher J, Moehl T, Kim Y J, Yi C, Comte P, Pei K, Holcombe T W, Nazeeruddin M K, Hua J, Zakeeruddin S M, Tian H, Grätzel M. Influence of the donor size in D-π-A organic dyes for dye-sensitized solar cells. Journal of the American Chemical Society, 2014, 136(15): 5722–5730
120. Zong X P, Liang M, Fan C R, Tang K, Li G, Sun Z, Xue S. Design of truxene-based organic dyes for high-efficiency dye-sensitized solar cells employing cobalt redox shuttle. Journal of Physical Chemistry C, 2012, 116(20): 11241–11250
121. Zong X, Liang M, Chen T, Jia J, Wang L, Sun Z, Xue S. Efficient iodine-free dye-sensitized solar cells employing truxene-based organic dyes. Chemical Communications, 2012, 48(53): 6645–6647
122. Xia Q, Liang M, Tan Y L, Gao W X, Ouyang L Y, Ge G Y, Sun Z, Xue S. Engineering of the electron donor of triarylamine sensitizers for high-performance dye-sensitized solar cells. Organic Electronics, 2015, 17: 285–294
123. Tsao H N, Yi C, Moehl T, Yum J H, Zakeeruddin S M, Nazeeruddin M K, Grätzel M. Cyclopentadithiophene bridged donor-acceptor dyes achieve high power conversion efficiencies in dye-sensitized solar cells based on the tris-cobalt bipyridine redox couple. ChemSusChem, 2011, 4(5): 591–594
124. Tsao H N, Burschka J, Yi C Y, Kessler F, Nazeeruddin M K, Grätzel M. Influence of the interfacial charge-transfer resistance at the counter electrode in dye-sensitized solar cells employing cobalt redox shuttles. Energy & Environmental Science, 2011, 4(12): 4921–4924
125. Yella A, Humphry-Baker R, Curchod B F E, Astani N A, Teuscher J, Polander L E, Mathew S, Moser J E, Tavernelli I, Rothlisberger U, Grätzel M, Nazeeruddin M K, Frey J. Molecular engineering of a fluorene donor for dye-sensitized solar cells. Chemistry of Materials, 2013, 25(13): 2733–2739
126. Polander L E, Yella A, Teuscher J, Humphry-Baker R, Curchod B F E, Astani N A, Gao P, Moser J E, Tavernelli I, Rothlisberger U, Grätzel M, Nazeeruddin M K, Frey J. Unravelling the potential for dithienopyrrole sensitizers in dye-sensitized solar cells. Chemistry of Materials, 2013, 25(13): 2642–2648
127. Zhang X, Mao J, Wang D, Li X, Yang J, Shen Z, Wu W, Li J, Ågren H, Hua J. Comparative study on pyrido[3,4-*b*]pyrazine-based sensitizers by tuning bulky donors for dye-sensitized solar cells. ACS Applied Materials & Interfaces, 2015, 7(4): 2760–2771
128. Li X, Zhou Y, Chen J, Yang J, Zheng Z, Wu W, Hua J, Tian H. Stacked graphene platelet nanofibers dispersed in the liquid electrolyte of highly efficient cobalt-mediator-based dye-sensitized solar cells. Chemical Communications, 2015, 51(51): 10349–10352
129. Yum J H, Holcombe T W, Kim Y, Rakstys K, Moehl T, Teuscher J, Delcamp J H, Nazeeruddin M K, Grätzel M. Blue-coloured highly efficient dye-sensitized solar cells by implementing the diketo-pyrrolopyrrole chromophore. Scientific Reports, 2013, 3: 2446
130. Yao Z, Zhang M, Wu H, Yang L, Li R, Wang P. Donor/acceptor indenoperylene dye for highly efficient organic dye-sensitized solar cells. Journal of the American Chemical Society, 2015, 137 (11): 3799–3802
131. Kakiage K, Aoyama Y, Yano T, Oya K, Kyomen T, Hanaya M. Fabrication of a high-performance dye-sensitized solar cell with 12.8% conversion efficiency using organic silyl-anchor dyes. Chemical Communications, 2015, 51(29): 6315–6317

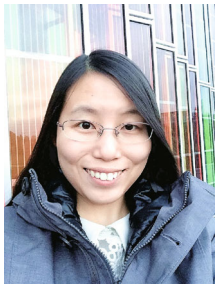

Xiaoyu Zhang received her Bachelor of Engineering with a major of Applied Chemistry in East China University of Science and Technology in 2011. Afterwards, she was specially recommended to a MS/PhD combined program and joined the research group of Prof. Jianli Hua at the Laboratory for Advanced Materials and Institute of Fine Chemicals in the same university. Currently, she is working in Prof. Micheal Grätzel's research group at École Polytechique Fédérale de Lausanne with the scholarship provided by China Scholarship Council. Her research interest is focused on the application of organic sensitizers on the solid-state and liquid-state dye-sensitized solar cells.

Michael Grätzel, Professor of Physical Chemistry at École Polytechnique Fédérale de Lausanne, he directs there the Laboratory of Photonics and Interfaces. He pioneered research in the field of energy and electron transfer reactions in mesoscopic systems and their exploitation for the generation of electricity and fuels from sunlight as well as the storage of electric power in lithium ion batteries. He is the inventor of dye sensitized solar cells that used for the first time 3-dimensional nanocrystalline junctions accomplishing very efficient harvesting of sunlight as well as photo-induced charge carrier separation and collection with near unity quantum yield. His research has engendered the advent of perovskite solar cells; one of the most exciting developments in the history of photovoltaics that have already reached over 20% solar to electric power conversion efficiencies. Author of several books and some 1100 publications that received over 165000 citations (H-factor 185), he is one of the three most highly cited chemists in the world. His recent awards include the King Feisal International Science Prize, Samson Prime Minister's Prize for Innovation in Alternative Fuels, First Leigh-Ann Conn Prize in Renewable Energy, Albert Einstein World Award of Science, Marcel Benoist Prize, Paul Karrer Gold Medal, Millennium Technology Grand Prize, and the Balzan Prize. He graduated as Doctor of natural science (Dr.rer.nat.) from the Technical University of Berlin and received 10 honorary doctors degrees from Asian and European Universities. He is a member of the Swiss Chemical Society and the German Academy of Science (Leopoldina) as well as a Honorary member of the Israeli Chemical Society, the Bulgarian Academy of Science, the European Academy of Science and the Société Vaudoise de Sciences Naturelles. Recently, he was named Fellow of the Max Planck Society and Honorary Fellow of the Royal Society of Chemistry (UK).

Jianli Hua received her Ph.D. degree from Wuhan University in 2002 under the supervision of Prof. Jingui Qin. She conducted her postdoctoral research at East China University of Science and Technology (ECUST) in Prof. He Tian's group in 2002 – 2004 and the Hong Kong University of Science & Technology in Prof. Ben Zhong Tang's group in 2004 – 2005. Prof. Hua became a full professor in 2002 and work at ECUST now. Her current research interests include the development of new molecules and polymers with novel structures and electronic and optical properties.